ACS OMEGA

http://pubs.acs.org/journal/acsodf

Article

Ring Distortion of Vincamine Leads to the Identification of Re-Engineered Antiplasmodial Agents

Verrill M. Norwood IV, Claribel Murillo-Solano, Michael G. Goertzen II, Beau R. Brummel, David L. Perry, James R. Rocca, Debopam Chakrabarti,* and Robert William Huigens III*

Cite This: *ACS Omega* 2021, 6, 20455−20470

Read Online

ACCESS | Metrics & More | Article Recommendations | Supporting Information

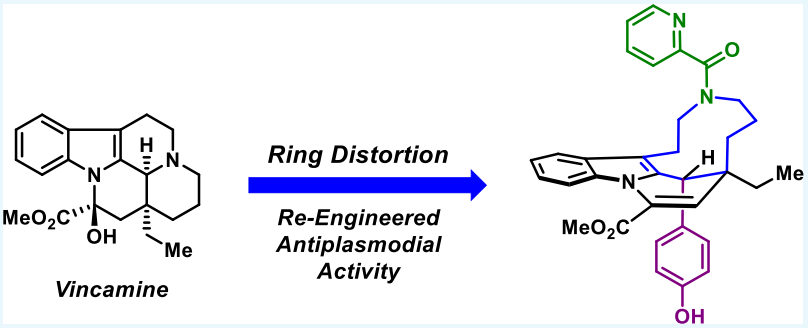

ABSTRACT: There is a significant need for new agents to combat malaria, which resulted in ∼409,000 deaths globally in 2019. We utilized a ring distortion strategy to create complex and diverse compounds from vincamine with the goal of discovering molecules with re-engineered biological activities. We found compound **8** (**V3b**) to target chloroquine-resistant *Plasmodium falciparum* Dd2 parasites (EC_{50} = 1.81 ± 0.09 μM against Dd2 parasites; EC_{50} > 40 μM against HepG2 cells) and established structure−activity relationships for 25 related analogues. New analogue **30** (**V3ss**, Dd2, EC_{50} = 0.25 ± 0.004 μM; HepG2, EC_{50} > 25 μM) was found to demonstrate the most potent activity, which prevents exit on the parasite from the schizont stage of intraerythrocytic development and requires >24 h to kill *P. falciparum* Dd2 cells. These findings demonstrate the potential that vincamine ring distortion has toward the discovery of novel antimalarial agents and other therapies significant to human health.

INTRODUCTION

Malaria is a global health problem caused by several *Plasmodium* parasites, with *Plasmodium falciparum* being the most deadly to humans.[1−3] The World Health Organization (WHO) estimated 229 million new cases and 409,000 deaths due to malaria in 2019.[4] Clinical agents used to treat malaria have been developed from drugs initially discovered more than 30 years ago and primarily belong to the artemisinin, aminoquinoline, or antifolate class.[5] Unfortunately, *P. falciparum* has developed resistance to each of these major drug classes,[6] and artemisinin-based combination therapies (ACTs) are becoming ineffective in several regions where malaria has reached epidemic proportions.[7,8] As such, there is a critical need for novel antimalarial agents that operate through unique modes of action to combat the widespread resistance to our current arsenal of drugs.[3,9−11]

Natural products have played a critical role in medicine due to their ability to bind and modulate cellular targets involved in disease.[12−15] Drug-target interactions that enable natural products to be effective therapies are dictated by structural features often involving complex molecular architectures that orient functional groups in space (*e.g.*, morphine,[16] vancomycin,[17] ecteinascidin 743,[18] and tetracycline[19]). There are many instances of synthetic analogues enhancing the inherent therapeutic benefit of a natural product; however, we are interested in re-engineering the biological activity of select natural products to explore novel molecular scaffolds in multiple disease areas. To do this, our group has established a ring distortion platform using indole alkaloids as starting points in synthesis pathways aimed to dramatically alter their inherently complex, fused ring systems to generate diverse molecular architectures that could bind alternative disease-relevant targets.[11,20−24]

Ring distortion of natural product efforts are distinct from other synthesis-driven discovery approaches, including diversity-oriented synthesis (DOS)[25−27] and biology-oriented synthesis (BIOS),[28,29] which rely on complexity-generating reactions of simple starting materials to rapidly access

Received: May 11, 2021
Accepted: June 22, 2021
Published: July 28, 2021

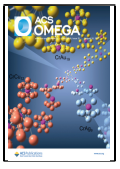

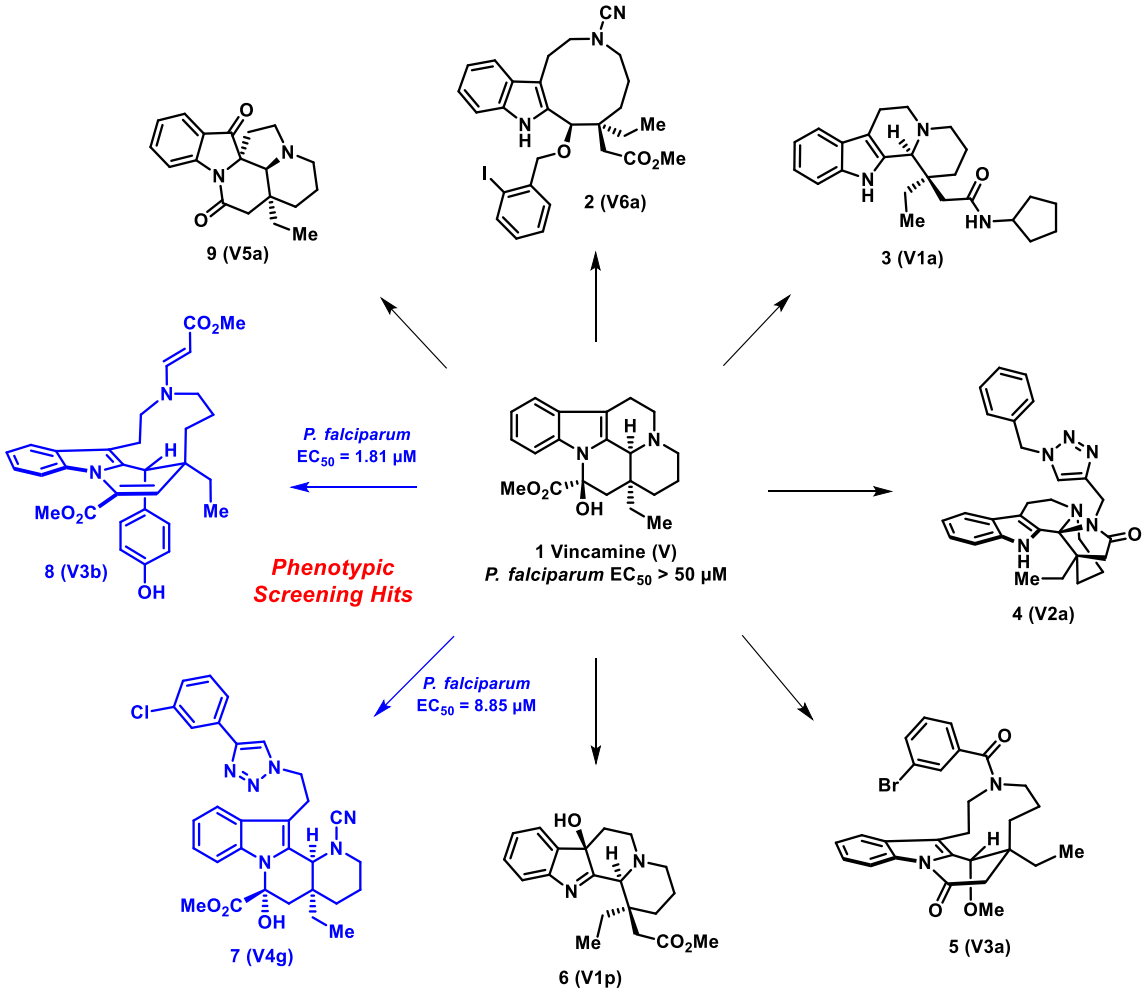

Figure 1. Complex and diverse scaffolds rapidly synthesized from vincamine. In this study, analogues **8** (**V3b**) and **7** (**V4g**) were identified as hit compounds demonstrating antiplasmodial activities against Dd2 parasites (note: vincamine does not have antiplasmodial activity).

compounds inspired by natural products. Each of these approaches (ring distortion of natural products, DOS, and BIOS) aim to generate diverse compound libraries to identify new small-molecule probes and/or hits for drug discovery,[30−32] and DOS efforts have resulted in the identification of promising antiplasmodial agents.[33−35]

Tactically, ring distortion efforts prioritize synthetic sequences involving ring cleavage, ring expansion, ring fusion, and ring rearrangement reactions applied to available complex natural products.[36−39] Our group has reported ring distortion efforts on yohimbine[20] and vincamine,[23] while others have successfully employed this approach on abietic acid,[40] adrenosterone,[36] gibberellic acid,[36] lycorine,[41] pleuromutilin,[39,42] quinine,[36] sinomenine,[43] and other steroidal systems.[38] Re-engineered biological activities from ring distortion efforts include (1) ferroptocide,[39] an anticancer agent produced from the antibiotic pleuromutulin, (2) **V2a**,[23] a compound that inhibits morphine-seeking behaviors in mice from vincamine, and (3) **Y7j**,[11] an antiplasmodial agent produced from yohimbine. In addition, we have shown that diverse compounds synthesized from vincamine and yohimbine display an array of unique antagonistic activity profiles against GPCRs of disease relevance, including cancer and addiction (168 GPCR panel at DiscoverX).[23,24]

Vincamine is a complex indole alkaloid commercially available on deca-gram scale (cost ∼$36 per gram) and utilized as a prescription medication (Oxybral SR) to improve cerebral blood flow and cognition. Vincamine demonstrates no activities against *P. falciparum*, which was shown during these studies (EC_{50} > 50 μM against chloroquine-resistant *P. falciparum* Dd2 parasites). Here, we performed a phenotypic screen to identify new antiplasmodial agents (EC_{50} < 1 μM against Dd2 cells) from our vincamine ring distortion library. In addition, we investigated structurally related analogues from our vincamine library and performed iterative rounds of chemical synthesis and *in vitro* testing to identify significantly more potent analogues with re-engineered antiplasmodial activities. We further evaluated the most potent analogue from this work, compound **30** (**V3ss**), to determine its developmental stage-specific action and kinetic kill rates against *P. falciparum*.

RESULTS AND DISCUSSION

Phenotypic Screen to Identify New Antiplasmodial Agents. We screened 80 diverse, vincamine-derived compounds synthesized using our ring distortion platform for antiplasmodial activity using chloroquine-resistant *P. falciparum* parasites (strain Dd2) in an unbiased cell-based SYBR Green I assay.[44−46] In this phenotypic screen, all compounds were evaluated at 2 μM (96-well format) and positive hits were determined at ≥40% inhibition of parasite growth. Results

https://doi.org/10.1021/acsomega.1c02480
ACS Omega 2021, 6, 20455−20470

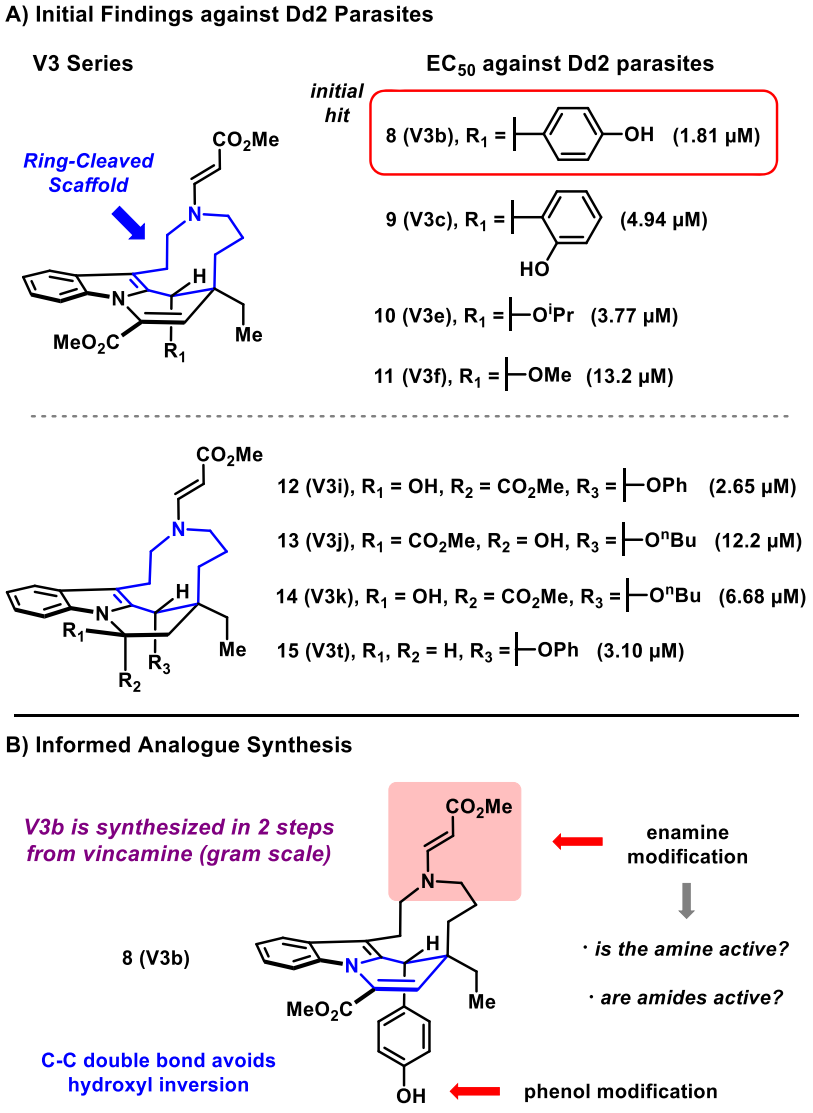

Figure 2. (A) Antiplasmodial activities of **V3** analogues from initial investigations with chloroquine-resistant *P. falciparum* parasites. (B) Future analogues were informed by initial antiplasmodial findings coupled to structural modifications of **8** (**V3b**) that could be probed with iterative rounds of synthesis and *in vitro* testing.

from the initial screen against Dd2 parasites indicated analogues **7** (**V4g**) and **8** (**V3b**) to be among the most active compounds (Figure 1). Follow-up dose−response experiments showed that these compounds had encouraging potencies with EC_{50} values of 8.85 ± 0.67 μM for **7** and 1.81 ± 0.09 μM for **8** against Dd2 cells [dose−response experiments were performed from freshly made dimethyl sulfoxide (DMSO) stock solutions of test compounds].

With analogue **8** (**V3b**) demonstrating encouraging potency against Dd2 parasites, we evaluated this compound against HepG2 (liver hepatocellular carcinoma) cells and found this agent to demonstrate no cytotoxicity (EC_{50} > 40 μM, highest test concentration). Based on the Dd2 parasite activity and HepG2 cytotoxicity profiles for **8**, the selectivity index (SI) for this initial hit is >22 (EC_{50} HepG2/EC_{50} Dd2) and we were very encouraged by this discovery. At this stage, we tested parent vincamine **1** at higher concentrations in dose−response experiments and found it to be inactive against Dd2 parasites (EC_{50} > 50 μM, highest test concentration). These results clearly demonstrate the antiplasmodial activity of **8** (EC_{50} = 1.81 ± 0.09 against Dd2, no cytotoxicity against HepG2) as "re-engineered" when compared to parent vincamine **1** (EC_{50} > 50 μM against Dd2).

Following the identification of analogue **8** (**V3b**), several structurally related **V3** analogues present in the initial vincamine ring distortion library (**9**/**V3c**, **10**/**V3e**, **11**/**V3f**, **12**/**V3i**, **13**/**V3j**, **14**/**V3k**, and **15**/**V3t**) were evaluated in dose−response experiments against Dd2 parasites to obtain initial structure−activity relationship (SAR) insights (Figure 2A). Structural diversity among the **V3** analogues included (1) variation at R_1 of **8**, **9**, **10**, and **11** or R_3 of **12**, **13**, **14**, and **15** bearing aryl or ether moieties or (2) functionalization of the six-membered ring fused to the indole nitrogen (carbon−carbon double bond in analogues **8**−**11**; α/β hydroxyl group in **12**−**14**; and complete reduction to the corresponding hydrocarbon in **15**). Despite the structural variation, each of these **V3** analogues displayed reduced activity against Dd2 (EC_{50} = 2.65−13.2 μM; Table 1) when compared to **8**.

The initial SAR showed that several modifications on the **V3** scaffold could be tolerated and guided our next-step plan of attack regarding analogue synthesis. We turned our focus to potential modifications of the enamine functional group

https://doi.org/10.1021/acsomega.1c02480
ACS Omega 2021, 6, 20455−20470

Table 1. Summary of Antiplasmodial Activities for V and V3/V4 Analogues[a]

cpd	code	EC_{50} Dd2 (μM)	EC_{50} 3D7 (μM)	EC_{50} HepG2 (μM)	selectivity index (SI)	stage-specific activity	kill rate
1	**V**	>50	>50	-	-	-	-
7	**V4g**	8.85 ± 0.67	-	-	-	-	-
8	**V3b**	1.81 ± 0.09	-	>40	>22	-	-
9	**V3c**	4.94 ± 0.26	-	-	-	-	-
10	**V3e**	3.77 ± 0.23	-	-	-	-	-
11	**V3f**	13.2 ± 0.67	-	-	-	-	-
12	**V3i**	2.65 ± 0.32	-	-	-	-	-
13	**V3j**	12.2 ± 0.23	-	-	-	-	-
14	**V3k**	6.68 ± 0.28	-	-	-	-	-
15	**V3t**	3.10 ± 0.29	-	-	-	-	-
18	**V3hh**	10.8 ± 2.93	-	-	-	-	-
19	**V3gg**	6.11 ± 1.56	-	-	-	-	-
20	**V3ii**	>20	12.0 ± 3.4	-	-	-	-
21	**V3jj**	0.63 ± 0.12	1.33 ± 0.18	-	-	-	-
22	**V3kk**	4.10 ± 0.55	-	-	-	-	-
23	**V3ll**	2.53 ± 0.34	-	-	-	-	-
24	**V3mm**	1.54 ± 0.004	-	-	-	-	-
25	**V3nn**	0.55 ± 0.07	2.25 ± 0.40	>25	>45	-	-
26	**V3oo**	2.48 ± 0.33	1.80 ± 0.36	>25	>10	-	-
27	**V3pp**	0.73 ± 0.11	1.99 ± 0.30	>25	>34	-	-
28	**V3qq**	2.14 ± 0.36	0.97 ± 0.03	>25	>11	-	-
29	**V3rr**	2.98 ± 0.40	3.18 ± 0.07	-	-	-	-
30	**V3ss**	0.25 ± 0.004	1.19 ± 0.25	>25	>100	late schizont	>24 h
31	**V3tt**	5.90 ± 0.26	-	-	-	-	-
32	**V3uu**	0.49 ± 0.10	2.22 ± 0.34	>25	>51	-	-
33	**V3vv**	0.65 ± 0.009	1.70 ± 0.32	>25	>38	-	-
34	**V3ww**	2.95 ± 1.14	6.60 ± 1.06	-	-	-	-

[a]The symbol "-" is for compounds not tested in a particular assay/experiment. The selectivity index (SI) was generated based on the relative activity between Dd2 and HepG2 cells [HepG2 EC_{50}/EC_{50} Dd2 cells]. All values reported in this table are the result of three, or more, independent experiments. Chloroquine was used as a comparator in dose−response experiments (Dd2, EC_{50} = 0.19 ± 0.01 μM; 3D7, EC_{50} = 0.017 ± 0.001).

present in all initial **V3** analogues (Figure 2B). We settled on using **8** (**V3b**) as a starting point for subsequent analogue synthesis and were curious to know (1) the requirements of the enamine group for antiplasmodial activity and (2) if we could readily transform the enamine to the corresponding amine and amide analogues to enhance the activity of **V3** analogues.

Chemical Synthesis of Vincamine-Derived Antiplasmodial Agents with SAR. Our initial efforts focused on scaling up the synthesis of **8** (**V3b**) as this antiplasmodial agent was the starting point for diversification. Using our previous chemistry,[23] we refluxed vincamine with *p*-toluenesulfonic acid in toluene to dehydrate **1** and form the corresponding α,β-unsaturated ester **16** (**V3ff**; 95% yield, 4.5 g; Figure 3A). Subsequent reaction of **16** with methyl propiolate in the presence of excess phenol resulted in indole-promoted C−N ring cleavage which afforded three products, including **8** (47% yield, 2.5 g isolated), **9** (5%), and **17** (12%). The three products from this reaction were readily separated *via* column chromatography and provided sufficient amounts of **8** for downstream chemistry and biological assessment.

Our ventures into understanding more about the SAR of **8** (**V3b**) involved two single-point transformations, including (1) acid-mediated hydrolysis of the enamine to amine **18** (**V3hh**, 77% yield) and (2) acylation of its phenolic hydroxyl to ester **19** (**V3gg**, 84% yield; Figure 3B) using acetic anhydride. Each transformation was insightful as amine analogue **18** showed a 6.0-fold loss in antiplasmodial activity (EC_{50} = 10.8 μM against Dd2 parasites; Figure 4 and Table 1), while acylated agent **19** reported a 3.4-fold loss in activity (EC_{50} = 6.11 μM) when compared to **8**.

Based on SAR findings with **18** and **19** (Figure 4), we were curious to evaluate **V3** analogues that replace the enamine moiety with amides and utilized **18** as the key synthetic intermediate for diversification. Collectively, we employed four amidation protocols using amine **18** and readily available acyl chlorides or carboxylic acids to generate 15 new amide analogues in 28−95% yield (Figure 3B). During this phase of our investigations, we carried out iterative rounds of synthesis (three to five new amide analogues) and *in vitro* testing against *P. falciparum* that served to inform the next round of analogue synthesis. Encouragingly, we found several amide analogues to demonstrate more potent antiplasmodial activities than **8**.

Our initial amidation efforts led to analogues **20** (**V3ii**)−**24** (**V3mm**) in 28−51% yield (Figure 3B). *In vitro* testing of these compounds against Dd2 parasites revealed that **21** (**V3jj**), an amide analogue bearing a pyridine heterocycle, has the most potent activity in this subseries (EC_{50} = 0.63 μM, Table 1) against *P. falciparum*. This insight guided the remainder of our synthesis, which prioritized heterocyclic amide analogues (pyridine, furan, pyrrole, isoxazole, and pyrimidine) for biological testing. Thus, **25** (**V3nn**)−**34** (**V3ww**) were synthesized in 30−95% yield; however, there were some cases of over acylation of the phenol group, which was remedied by a one-pot, two-step ester saponification with potassium carbonate in methanol.

Collectively, six amide analogues reported good antiplasmodial activities against Dd2 parasites with EC_{50} values ≤0.8 μM

https://doi.org/10.1021/acsomega.1c02480
ACS Omega 2021, 6, 20455−20470

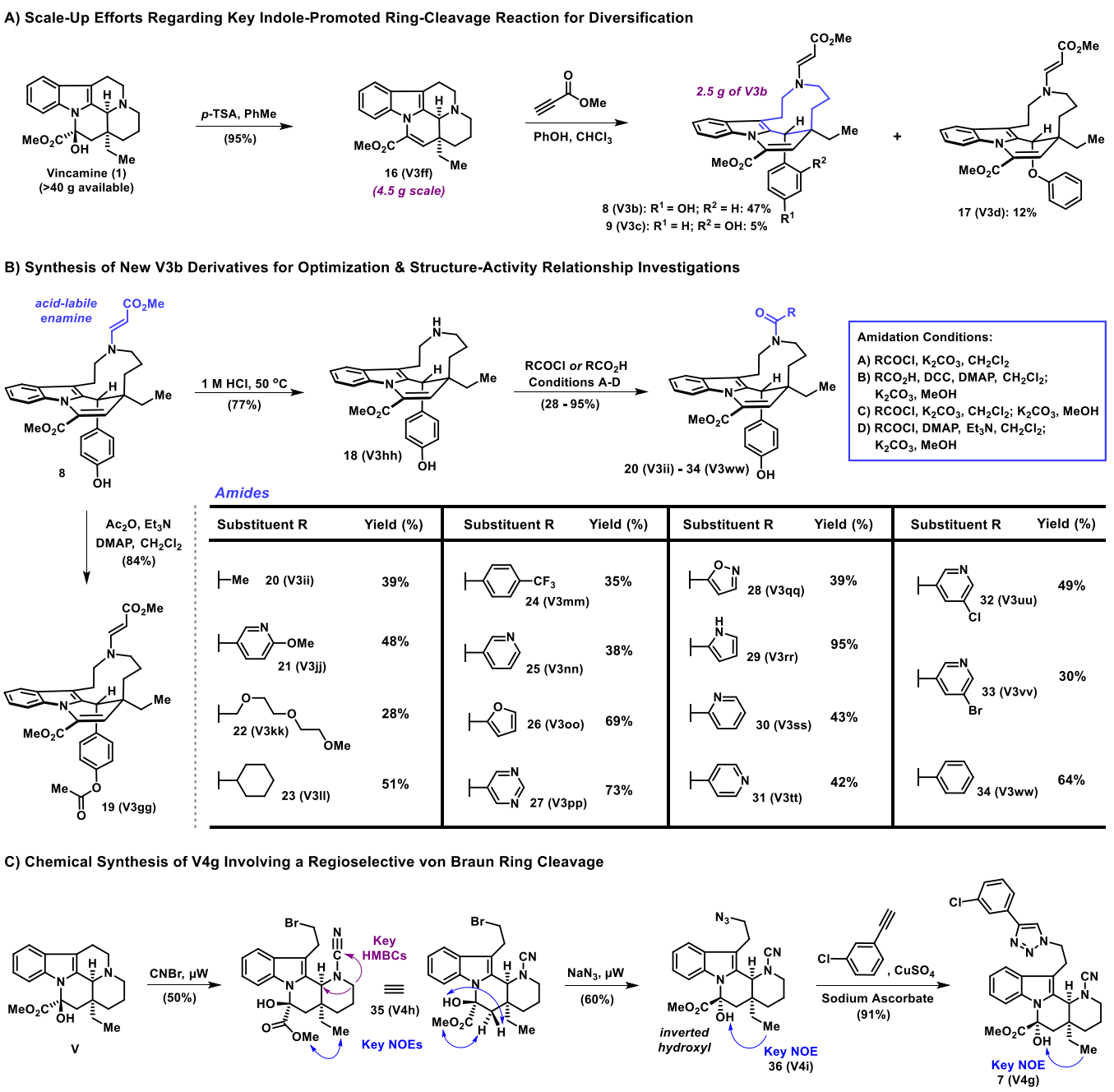

Figure 3. (A) Scale-up efforts to key ring-cleaved building block **8** (**V3b**). (B) Chemical synthesis of **V3** analogues for initial optimization and to establish an SAR profile. (C) Chemical synthesis of **7** (**V4g**).

(Table 1), including **30** (**V3ss**, EC_{50} = 0.25 ± 0.004 μM), **32** (**V3uu**, EC_{50} = 0.49 ± 0.10 μM), **25** (**V3nn**, EC_{50} = 0.55 ± 0.07 μM), **21** (**V3jj**, EC_{50} = 0.63 ± 0.12 μM), **33** (**V3vv**, EC_{50} = 0.65 ± 0.009 μM), and **27** (**V3pp**, EC_{50} = 0.73 ± 0.11 μM). Several amide analogues were advanced to cytotoxicity testing against HepG2 cells and were found to have minimal activities at the highest test concentration of 25 μM (EC_{50} > 25 μM, Table 1). SIs were then generated based on HepG2 cytotoxicity (EC_{50})/Dd2 parasite activity (EC_{50}), which demonstrated **30** (SI > 100), **32** (SI > 51), and **25** (SI > 45) to have ideal plasmodial targeting. In addition, several new amide analogues were evaluated against wild-type *P. falciparum* 3D7 cells, and we found this strain to display lower levels of sensitivity to most amide analogues (*e.g.*, **30**/**V3ss**, EC_{50} = 1.19 ± 0.25 μM against 3D7 cells; Table 1), which was unexpected and we are actively looking further to understand the reason.

We present a focused SAR from initial hit **8** (**V3b**) to key analogues that led to our most potent agent **30** (Figure 4). Several amide analogues significantly improved antiplasmodial activities when compared to amine **18**. Several pyridinyl amide analogues (**21**/**V3jj**, **25**/**V3nn**, **30**/**V3ss**, and **31**/**V3tt**) gave insights into nitrogen placement relative to the amide moiety to find that the nitrogen *ortho* (**30**) and *meta* (**21** and **25**) were significantly more active than when the nitrogen atom was placed *para* (**31**). Analogue **34** (**V3ww**) has a phenyl amide and demonstrates that the removal of the nitrogen atom from the aromatic moiety also reduces activity compared to the pyridinyl analogues with a nitrogen atom in the *ortho*- and *meta*-positions. Upon further analysis, cyclohexyl amide **23** and

https://doi.org/10.1021/acsomega.1c02480
ACS Omega 2021, 6, 20455−20470

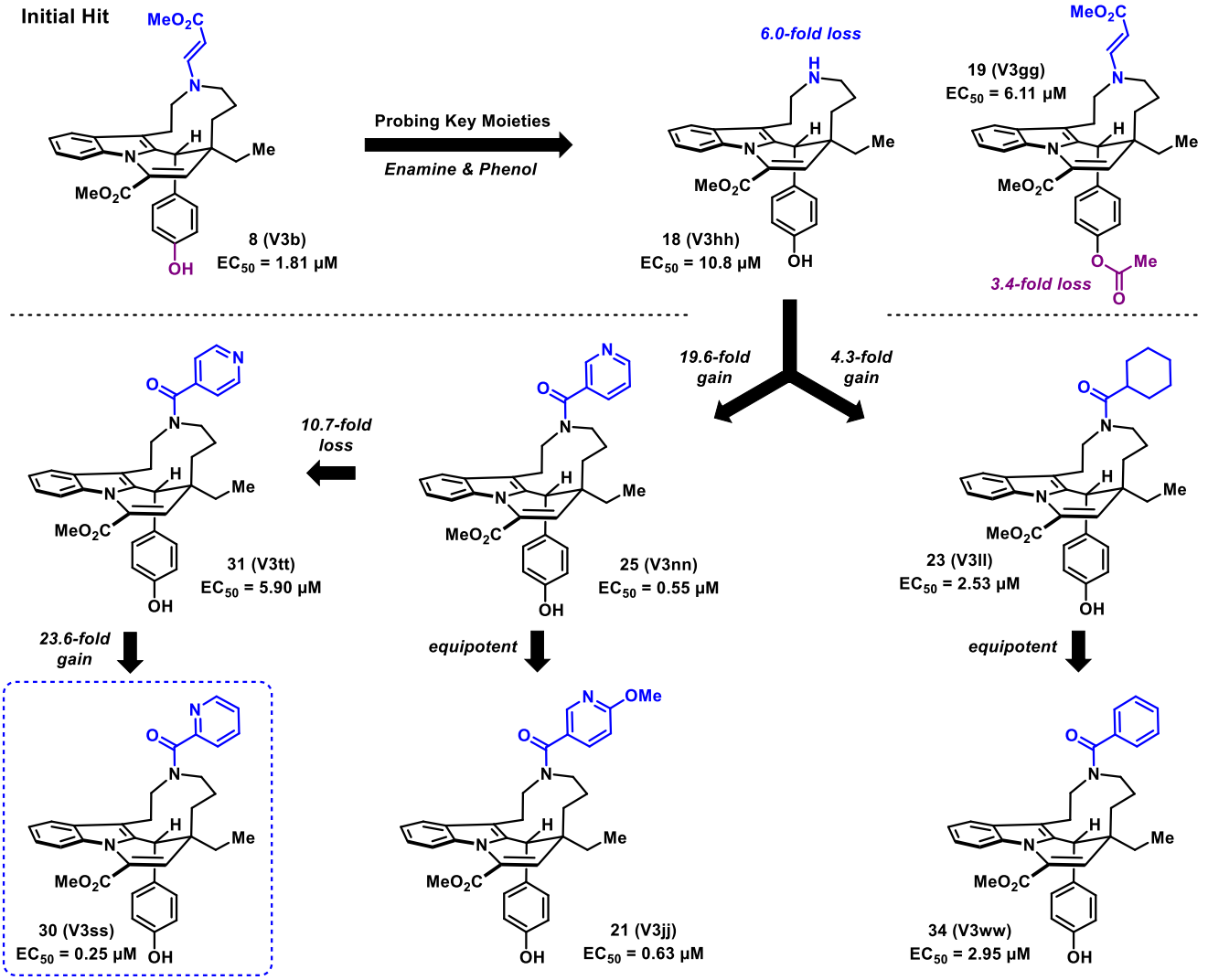

Figure 4. Detailed SAR profiles regarding the **V3** antiplasmodial agents.

34 had improved potencies against Dd2 parasites compared to pyridine analogue **31** bearing the nitrogen *para* to the amide group, demonstrating that a nitrogen in this position significantly reduces activity in this analogue series.

In addition to analogue **30** (**V3ss**) demonstrating good antiplasmodial activities against resistant *P. falciparum* parasites, we determined some solubility and chemical stability properties. For solubility, we found **30** to readily dissolve in DMSO to make a 100 mM solution (highest concentration tested). Additionally, phosphate-buffered saline (PBS) was slowly titrated into a 10 mM DMSO stock of **30** to make a final 100 μM aqueous solution which was completely soluble at room temperature by visual inspection (500 μL aliquot). To determine chemical stability, we prepared solutions of **30** in PBS buffer at pH 2.0 and 7.4 (physiologically relevant) and allowed this agent to incubate for 24 h at room temperature and then for an additional 24 h at 37 °C. After each 24 h time point, stability was determined by TLC analysis to show no compound breakdown (see Supporting Information), which was also confirmed by NMR analysis. For additional insights regarding chemical stability, all NMR experiments of **30** (and related analogues) were conducted at 100 °C for multiple hours without showing compound breakdown. Overall, we found the solubility properties and chemical stability of analogue **30** to be quite good.

In addition to **V3** amide analogues, we found **7** (**V4g**) to display antiplasmodial activity against Dd2 parasites. Compound **7** (**V4g**) was synthesized from vincamine using a three-step sequence that involved (1) a microwave-mediated, regioselective von Braun ring cleavage of **1** using cyanogen bromide to give **35** (determined by HMBC and extensive NOEs, 50% yield; Figure 3C and Supporting Information), (2) sodium azide displacement of the primary bromide in **35** that readily gave azide **36** under microwave heating in *N*,*N*-dimethylformamide (DMF) and was accompanied by an unexpected inversion of the hydroxyl group as determined by NOE (60% yield), and (3) a final click reaction of **36** with 1-chloro-3-ethynylbenzene that gave **7** (**V4g**) in 91% yield. Analogues of **7** were not pursued further, so we could focus our efforts on the more potent **V3** amide derivatives; however, **7** (**V4g**) could be a starting point for future endeavors regarding vincamine-derived antiplasmodial agents.

Developmental Stage-Specific Action for Analogue 30 (V3ss). Elucidation of the developmental stage in the intraerythrocytic life cycle at which antiplasmodial agents act can provide critical insights into potential modes of action and clinical clearance of the parasite. To further probe the

https://doi.org/10.1021/acsomega.1c02480
ACS Omega 2021, 6, 20455−20470

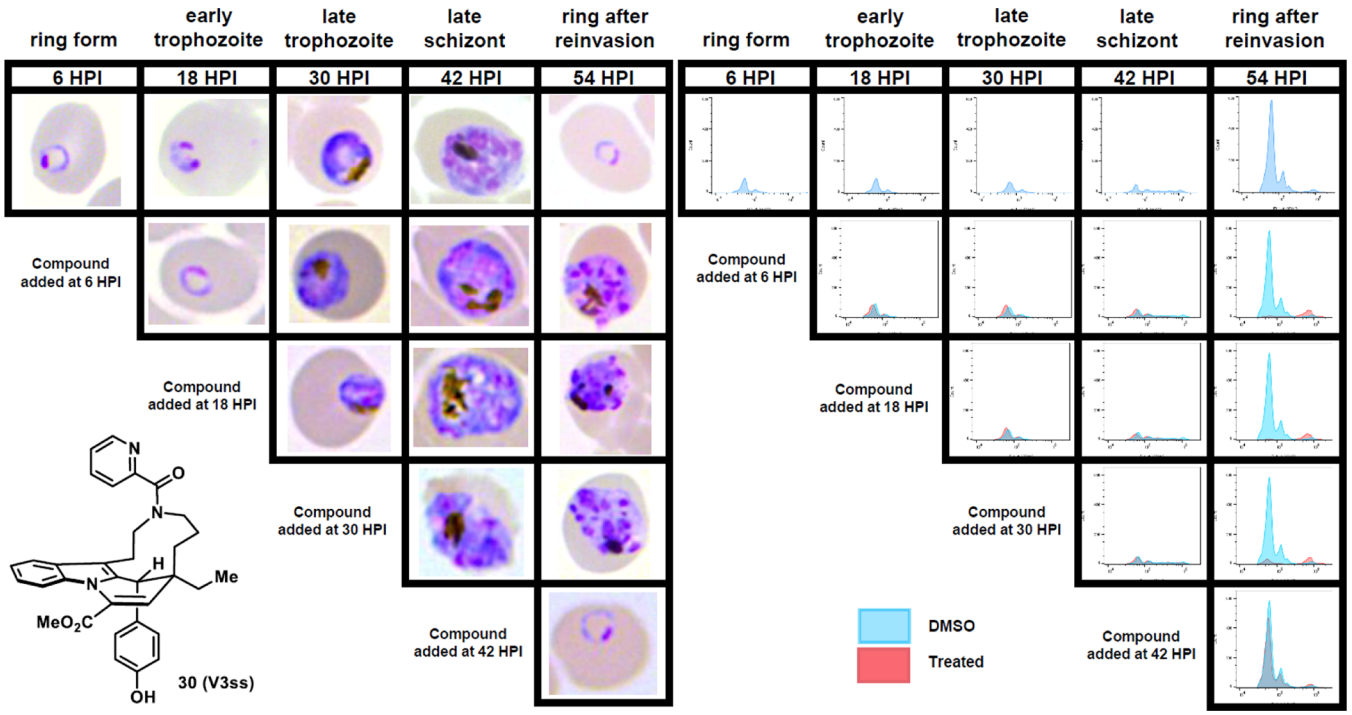

Figure 5. Stage-specific activity of **30** (**V3ss**) in *P. falciparum* Dd2 cells. Tightly synchronized Dd2 cultures were treated with 5 x EC_{50} of **30** at 6, 18, 30, and 42 HPI. Blood smears and Giemsa staining were taken at each time point as well to verify the phenotype. Flow cytometry was performed to quantify the stage of action for **V3ss** at the time of harvesting, following 6, 18, 30, and 42 HPI treatments. For flow cytometry analysis, collected samples were fixed in a freshly prepared solution of 4% paraformaldehyde and 0.0075% glutaraldehyde, permeabilized with 0.25% Triton X-100, treated with RNase (50 μg/mL), and stained with YOYO-1. Data acquisition was performed in a CytoFLEX (Beckman) flow cytometer. DHA and atovaquone were evaluated as positive controls in stage-specific activity assays, and results from these experiments can be viewed in Supporting Information. Parasites following exposure to **30** (**V3ss**) are arrested at the late schizont stage.

antiplasmodial activity of **30** (**V3ss**), we evaluated its developmental stage-specific action using microscopy and flow cytometry (Figure 5).[47,48] The delineated timing of action was determined using tightly synchronized *P. falciparum* Dd2 cells treated with **30** (1.25 μM; 5X EC_{50} concentration) at 6, 18, 30, and 42 h postinvasion (HPI) of erythrocytes by merozoites. Following this, microscopic evaluation of Giemsa-stained smears and flow cytometric assessments were conducted at 12 h intervals.

Infected red blood cells treated with 0.1% DMSO served as negative controls in these experiments and this culture matured as expected through the trophozoite/schizont (30 HPI) and segmenter (42 HPI) stages and reappears as rings after reinvasion (54 HPI) with a concurrent increase in parasitemia (determined by flow cytometry, Figure 5). *P. falciparum* Dd2 cells treated with **30** (**V3ss**) at 6, 18, and 30 HPI progress into nuclear division and, however, do not advance beyond the late schizont stage (Figure 5). In addition, Dd2 cells treated with **30** at 6, 18, and 30 HPI showed a remarkable decrease in parasitemia (flow cytometry). Parasites treated at 42 HPI did not inhibit maturation through the remainder of the development cycle (Figure 5). Collectively, based on microscopy and flow cytometry findings, we conclude that the antiplasmodial action of **30** occurs specifically on the exit from the schizont stage.[49]

Killing Kinetics for Analogue 30 (V3ss). A series of kinetic kill experiments were performed in Dd2 cultures to determine if **30** (**V3ss**) elicits its antiplasmodial activities through a parasitocidal or parasitostatic mechanism (Figure 6). To conduct this, we treated asynchronous parasite cultures with **30** (5× EC_{50} concentration) for 6, 12, 24, and 48 h. Following each of these time points, the compound was washed out and parasite growth of the Dd2 cultures was evaluated for 96 h. Results from these kinetic kill experiments show that **30** reduces parasitemia after 24 h treatment (based on the 96 h time point, Figure 6C); however, there is a more dramatic parasitocidal effect after 48 h treatment with this compound (Figure 6D). From these experiments, we conclude that **30** is a (slow-killing) parasitostatic agent that displays a kinetic kill profile similar to atovaquone, a clinically used antiplasmodial agent (comparator with parasitostatic activity; Figure 6).

CONCLUSIONS

In conclusion, our vincamine ring distortion efforts to produce a unique and diverse library of complex small molecules have resulted in new antiplasmodial agents. As vincamine has no antiplasmodial activities (EC_{50} > 50 μM against Dd2 parasites), ring-distorted agents such as **30**/**V3ss** (EC_{50} = 0.25 ± 0.004 μM against Dd2) display re-engineered biological activities against deadly parasites, which is an ultimate goal of this program. We detail SAR profiles of **V3** agents from 25 structurally related analogues, including 17 new ring-cleaved compounds synthesized during these efforts. This new series of compounds displayed good plasmodial targeting with six analogues reporting an $EC_{50} \leq 0.8$ μM against Dd2 parasites while demonstrating minimal cytotoxicity against HepG2 cells (EC_{50} > 25 μM; SI > 100 for **V3ss**). Analogue **30**/**V3ss** was also shown to act specifically on the trophozoite/schizont stage and required >24 h treatment to eradicate *P. falciparum* Dd2 parasites in kill kinetic experiments. Future studies aim to

https://doi.org/10.1021/acsomega.1c02480
ACS Omega 2021, 6, 20455−20470

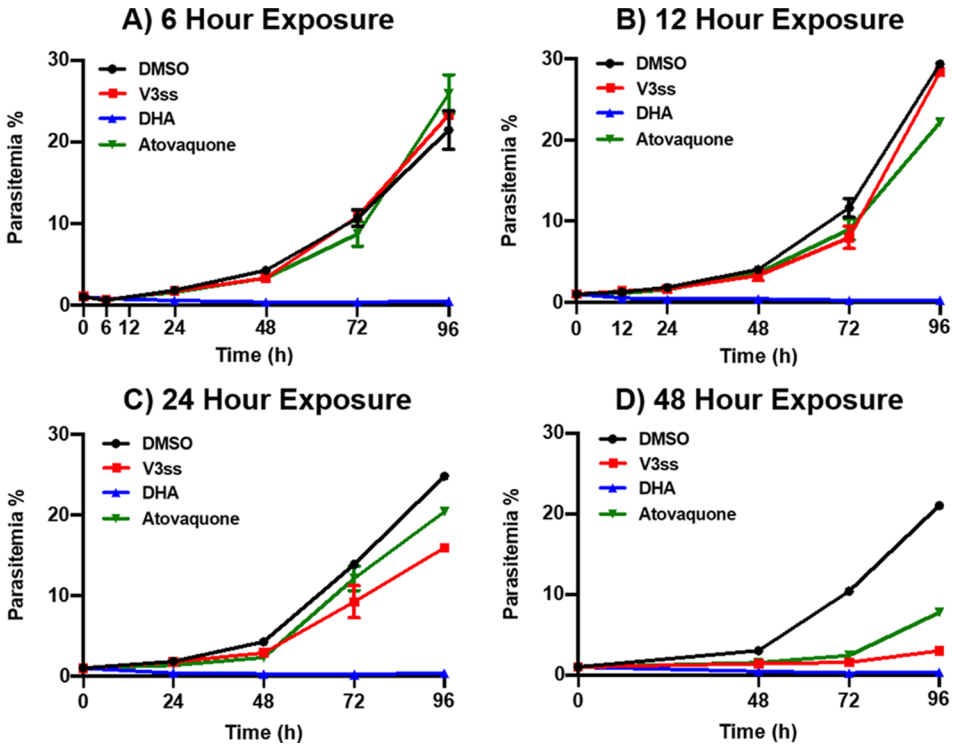

Figure 6. Kinetic kill experiments used to determine parasitocidal/parasitostatic activity of **30**/**V3ss** in *P. falciparum* Dd2 cultures. Asynchronous cultures were treated with **30** at 5 × EC_{50} for (A) 6, (B) 12, (C) 24, and (D) 48 h. Following each treatment, cultures were washed three times in RPMI, then resuspended in culture media, and monitored daily for parasite growth. Note: Dihydroartemisinin (DHA) was used as a positive control for rapid parasite killing (5 × EC_{50} = 50 nM) and atovaquone was used as a positive control for slow parasite killing (5 × EC_{50} = 6.6 nM) in these experiments. DMSO concentration was 0.15% in kinetic kill experiments.

determine the mode of action regarding V3 analogues and advance these agents to additional hit-to-lead optimization efforts to improve potency and mitigate any metabolic liabilities (*i.e.*, phenol moiety). Our vincamine ring distortion platform has led to the discovery of new re-engineered antiplasmodial agents, and we aim to further develop these agents to combat malaria.

EXPERIMENTAL SECTION

All reactions were carried out under an atmosphere of argon unless otherwise specified. Chemical reagents were purchased from commercial sources and used without further purification. Vincamine was purchased from AK Scientific at >98% purity (~$36 per gram during these studies). Anhydrous solvents were transferred *via* a syringe to flame-dried glassware, which was cooled under a stream of dry argon. Analytical thin-layer chromatography (TLC) was performed using 250 μm silica gel 60 F254 precoated plates (EMD Chemicals Inc). Flash column chromatography was performed using 230−400 Mesh 60 Å silica gel (Sorbent Technologies).

NMR experiments were recorded on the following instruments: Varian Unity spectrometer (400 MHz for ^{1}H NMR; 101 MHz for ^{13}C NMR), Bruker Avance III spectrometer (500 MHz for ^{1}H NMR; 126 MHz for ^{13}C NMR), Bruker AVANCE II spectrometer (600 MHz for ^{1}H NMR; 151 MHz for ^{13}C NMR), and Agilent Systems VNMRS spectrometer (600 MHz for ^{1}H NMR; 151 MHz for ^{13}C NMR). All spectra are presented using MestReNova 11.0 (Mnova) software and are displayed without the use of the signal suppression function. Spectra were obtained in the following solvents (reference peaks also included for ^{1}H and ^{13}C NMRs): $CDCl_3$ (^{1}H NMR: 7.26 ppm; ^{13}C NMR: 77.23 ppm) and $C_2D_2Cl_4$ (^{1}H NMR: 6.00 ppm; ^{13}C NMR: 73.78 ppm). NMR samples where the respective solvent peaks were buried in the sample signals referenced TMS at 0.00 ppm for ^{1}H NMR experiments. Chemical shift values (δ) are reported in parts per million (ppm) for all ^{1}H NMR and ^{13}C NMR spectra. ^{1}H NMR multiplicities are abbreviated and reported as follows: s = singlet, d = doublet, t = triplet, q = quartet, p = pentet, m = multiplet, and br = broad. Temperatures of NMR experiments are indicated with tabulated data, and several compounds required elevated temperatures to obtain publishable spectra.

NMR Dynamics of V3 Series: NMR spectra were recorded at 100 °C for amide analogues **20 (V3ii)**−**34 (V3ww)**. Based on variable temperature NMR experiments with **21**/**V3jj** (Supporting Information Figure 2) and other select analogues, we believe that **V3** series amide analogues are slowly interconverting conformers (as observed at room temperature). Many sharp signals for **V3** amide analogues can be observed at 100 °C. However, some ^{1}H and ^{13}C nuclei remain very broad or not visible in our spectra (including 2-D NMR experiments, which are included in Supporting Information). Similar phenomena in medium-sized ring systems have been reported in the literature.[50−52]

Melting points were obtained on a Mel-Temp II capillary melting point apparatus and were uncorrected. High-resolution mass spectra (HRMS) were obtained from the Mass Spectrometry Facility in the Chemistry Department at the University of Florida. Optical rotations were acquired on a Perkin Elmer Polarimeter 341, and concentrations were adjusted and reported as g/100 mL. Compound structures

https://doi.org/10.1021/acsomega.1c02480
ACS Omega 2021, 6, 20455−20470

were converted into IUPAC names using MarvinSketch (ChemAxon; Cambridge, MA).

The purities of all compounds evaluated in biological assays were confirmed to be ≥95% by LC−MS using a Shimadzu Prominence HPLC system, an AB Sciex 3200 QTRAP spectrometer, and a Kinetex EVO C18 column (50 mm × 2.1 mm × 2.6 μm) with a 30-min linear gradient from 10−95% acetonitrile in water at a flow rate of 0.20 mL/min. All biological experiments, including antiplasmodial screening with Dd2 parasites, dose−response assays with Dd2 and 3D7 strains, stage-specific activity assays, kill kinetics, and HepG2 (liver) cytotoxicity assays, were performed using protocols previously reported by the Chakrabarti lab.[48]

Chemical Synthesis Procedures and Characterization of New Compounds. *Synthesis of* ***7*** *(**V4g**).* Anhydrous copper sulfate (3.0 mg, 0.017 mmol) and sodium ascorbate (16.4 mg, 0.053 mmol) were added to a vial and dissolved in a solution of 0.9 mL of *tert*-butanol/water (1:2). The resulting mixture was then added to a round-bottom flask containing compound **36** (**V4i**; 24.1 mg, 0.06 mmol). Following this, 3-chloro-1-ethynylbenzene (9.70 μL, 0.11 mmol) was added dropwise to the reaction mixture as a 0.3 M solution in dichloromethane. The reaction mixture was vigorously stirred at room temperature for 1.5 h, and upon completion, the biphasic mixture was quenched with brine. The crude mixture was then extracted with dichloromethane, and the organic layer was subsequently collected, dried with sodium sulfate, filtered, and concentrated *in vacuo*. Finally, the crude product was purified *via* column chromatography using a gradient of 83:17 hexanes/ethyl acetate to 100% ethyl acetate to afford **7** (**V4g**) as a white solid (18.2 mg, 91%). ^{1}H NMR (400 MHz, $CDCl_3$): δ 7.64 (m, 1H), 7.54−7.47 (m, 2H), 7.35 (s, 1H), 7.29−7.12 (m, 5H), 4.94 (ddd, *J* = 13.5, 6.1, 4.1 Hz, 1H), 4.72 (s, 1H), 4.68 (m, 1H), 3.81 (s, 3H), 3.78 (d, *J* = 1.1 Hz, 1H), 3.63−3.50 (m, 2H), 3.44 (m, 1H), 3.20 (td, *J* = 12.7, 3.3 Hz, 1H), 2.85 (d, *J* = 14.3 Hz, 1H), 1.86−1.73 (m, 3H), 1.69−1.57 (m, 2H), 1.36−1.19 (m, 2H), 0.68−0.57 (m, 3H). ^{13}C NMR (101 MHz, $CDCl_3$): δ 174.4, 146.4, 135.2, 135.0, 132.7, 130.2, 128.6, 128.2, 128.1, 126.1, 124.1, 124.0, 121.6, 121.3, 119.3, 116.6, 113.5, 111.6, 82.4, 57.9, 54.6, 51.0, 50.5, 35.2, 35.0, 33.0, 30.3, 26.2, 20.4, 7.1. HRMS (ESI): calcd for $C_{30}H_{31}ClN_6O_3Na$ $[M + Na]^+$, 581.2038; found, 581.2030. mp 101−103 °C. $[\alpha]_{20}^{D}$ −6° (*c* 0.90 g/100 mL, CH_2Cl_2).

Synthesis of ***18*** *(**V3hh**), Methyl (11S,19S)-11-ethyl-19-(4-hydroxyphenyl)-8,15-diazatetracyclo[9.6.2.0^{2,7}.0^{8,18}]-nonadeca-1(18),2(7),3,5,9-pentaene-9-carboxylate.* Compound **8** (1.51 g, 2.94 mmol) was added to a stirring solution of 1 M hydrogen chloride solution in methanol (10 mL). The reaction mixture was then slowly warmed to 50 °C and allowed to stir for 26 h. Upon completion, the reaction was quenched with brine and extracted with ethyl acetate. The organic layer was collected, dried with sodium sulfate, filtered, and concentrated *in vacuo*. The crude material was then purified *via* column chromatography using a gradient of 99:1 chloroform/triethylamine to 96:3:1 chloroform/methanol/triethylamine to afford amine **18** (852 mg, 66%) as white foam. ^{1}H NMR (600 MHz, $CDCl_3$): δ 7.47 (d, *J* = 7.7 Hz, 1H), 7.26 (d, *J* = 8.2 Hz, 1H), 7.20 (ddd, *J* = 8.4, 6.8, 1.2 Hz, 1H), 7.14 (dd, *J* = 8.5, 7.6 Hz, 1H), 6.95 (d, *J* = 8.6 Hz, 2H), 6.58 (d, *J* = 8.6 Hz, 2H), 6.21 (d, *J* = 1.2 Hz, 1H), 4.47 (s, 1H), 4.00 (s, 3H), 3.11 (ddd, *J* = 12.6, 12.2, 4.4 Hz, 1H), 3.07−2.92 (m, 3H), 2.85 (m, 1H), 2.73 (m, 1H), 1.75 (dd, *J* = 15.1, 13.6 Hz, 1H), 1.63 (sextet, *J* = 7.3 Hz, 1H), 1.55 (m, 1H), 1.46 (ddd, *J* = 15.7, 7.2, 2.0 Hz, 1H), 1.26 (m, 1H), 0.89 (t, *J* = 7.4 Hz, 3H), 0.64 (dd, *J* = 15.0, 13.7 Hz, 1H). ^{13}C NMR (151 MHz, $CDCl_3$): δ 164.5, 155.9, 138.0, 135.6, 130.7, 130.5, 130.0, 128.9, 128.6, 122.9, 121.2, 119.0, 115.4, 112.3, 110.2, 52.9, 46.0, 45.0, 44.7, 44.4, 26.5, 25.8, 22.5, 21.5, 8.2. HRMS (ESI): calcd for $C_{27}H_{31}N_2O_3$ $[M + H]^+$, 431.2329; found, 431.2346. mp 190−192 °C. $[\alpha]_{20}^{D}$ −35° (*c* 0.26 g/100 mL, CH_2Cl_2). Note: COSY, TOCSY, and HSQC with key correlations highlighted of **18** (**V3hh**) can be viewed in the spectra section of the Supporting Information.

Synthesis of ***19*** *(**V3gg**), Methyl (11S,19S)-19-[4-(acetyloxy)phenyl]-11-ethyl-15-[(1E)-3-methoxy-3-oxoprop-1-en-1-yl]-8,15-diazatetracyclo[9.6.2.0^{2,7}.0^{8,18}]nonadeca-1-(18),2(7),3,5,9-pentaene-9-carboxylate.* Compound **8** (112 mg, 0.217 mmol) was added to a flame-dried round-bottom flask and then dissolved in anhydrous dichloromethane (3.3 mL). The solution was then cooled to 0 °C before triethylamine (30 μL, 0.217 mmol) and a catalytic 4-dimethylaminopyridine (DMAP, one crystal) were added sequentially. Following this, acetic anhydride (21 μL, 0.217 mmol dissolved in 1 mL of anhydrous dichloromethane) was added dropwise to the reaction mixture. The resulting mixture slowly warmed to room temperature over an hour. Upon completion by TLC, the reaction was quenched with saturated aqueous brine and extracted with dichloromethane. The combined organic layers were dried with sodium sulfate, filtered, and concentrated *in vacuo* to give the crude material that was purified *via* column chromatography using a gradient of 100% hexanes to 2:1 hexanes/ethyl acetate to afford **19** (104 mg, 86%) as a colorless residue. ^{1}H NMR (600 MHz, $CDCl_3$ at 50 °C): δ 7.66 (d, *J* = 13.3 Hz, 1H), 7.43 (d, *J* = 7.6 Hz, 1H), 7.24 (d, *J* = 8.1 Hz, 1H), 7.21 (ddd, *J* = 8.4, 7.6, 1.2 Hz, 1H), 7.16 (ddd, *J* = 8.1, 6.9, 1.3 Hz, 1H), 7.10 (d, *J* = 8.7 Hz, 2H), 6.93 (d, *J* = 8.6 Hz, 2H), 6.17 (s, 1H), 4.84 (d, *J* = 13.4 Hz, 1H), 4.24 (s, 1H), 4.00 (s, 3H), 3.77 (m, 1H), 3.75 (s, 3H), 3.56 (dd, *J* = 14.5, 7.3 Hz, 1H), 3.14 (dd, *J* = 15.8, 13.7 Hz, 1H), 3.02 (dd, *J* = 14.9, 12.7 Hz, 1H), 2.75 (br d, *J* = 13.1 Hz, 1H), 2.56 (dd, *J* = 14.4, 8.7 Hz, 1H), 2.24 (s, 3H), 1.83 (br dd, *J* = 15.6, 13.3 Hz, 1H), 1.69 (m, 1H), 1.46 (sextet, *J* = 7.3 Hz, 1H), 1.33 (m, 1H), 1.05 (sextet, *J* = 7.3 Hz, 1H), 0.96 (m, 1H), 0.85 (t, *J* = 7.4 Hz, 3H). ^{13}C NMR (151 MHz, $CDCl_3$ at 50 °C): δ 169.7, 169.4, 164.4, 151.2, 149.9, 137.3, 136.0, 135.2, 130.6, 130.3, 129.0, 128.7, 122.8, 121.5, 121.1, 118.1, 113.4, 112.3, 87.5, 59.3, 56.8, 52.8, 50.8, 45.9, 43.4, 34.4, 27.3, 21.9, 21.2, 8.3. Note: One aliphatic ^{13}C was not visible in this spectra. HRMS (ESI): calcd for $C_{33}H_{37}N_2O_6$ $[M + H]^+$, 557.2646; found, 557.2658. $[\alpha]_{20}^{D}$ −67° (*c* 0.34 g/100 mL, CH_2Cl_2).

General Amidation Procedure A. To a stirring solution of amine **18** (**V3hh**, 1.0 equiv) in anhydrous dichloromethane (0.05 M) at 0 °C was added potassium carbonate (1−2 equiv). Next, acyl chloride (1.0 equiv) was added to the mixture dropwise, and the resulting reaction mixture was stirred at 0 °C for 1 to 3 h (select reactions warmed to room temperature and were allowed to stir overnight). Upon completion (by TLC), the reaction was quenched with brine and extracted with dichloromethane. The combined organic layers were then dried with sodium sulfate, and the crude product was then purified by silica gel chromatography.

General Amidation Procedure B. Dicylcohexylcarbodiimide (1.0 equiv) was added at 0 °C to a stirring solution of amine **18** (**V3hh**, 1.0 equiv) dissolved in anhydrous dichloromethane (0.05 M). DMAP (one crystal) and carboxylic acid (1.0 equiv)

https://doi.org/10.1021/acsomega.1c02480
ACS Omega 2021, 6, 20455−20470

were then sequentially added, and the mixture was allowed to warm to room temperature slowly and continued to stir for 24 h. Upon completion of the reaction (by TLC), the contents of the mixture were filtered through a fritted funnel, and the resulting filtrate was concentrated *in vacuo*. The dried filtrate was then dissolved in a (1:1) 10% w/v aqueous potassium bicarbonate/methanol solution (0.3 M) and allowed to stir at room temperature for 12 h. After this time, the reaction was quenched with brine and extracted with dichloromethane. The combined organic layers were then dried with sodium sulfate, and the crude material was purified by silica gel chromatography.

General Amidation Procedure C. Potassium carbonate (1.0−2.0 equiv) was added at 0 °C to a stirring solution of amine **18** (**V3hh**, 1.0 equiv) in anhydrous dichloromethane (0.05 M). Acyl chloride (1.0 equiv) was then added dropwise, and the resulting mixture was allowed to stir at 0 °C for 1 to 3 h. Upon completion of the reaction (by TLC), the mixture was concentration *in vacuo*, dissolved in a (1:1) 10% w/v aqueous potassium bicarbonate/methanol solution (0.3 M), and allowed to stir at room temperature for 3 to 12 h. After this time, this second reaction was quenched with brine and extracted with dichloromethane. The organic layers were then combined and dried with sodium sulfate to give a crude product, which was purified by silica gel chromatography.

General Amidation Procedure D. Triethylamine (2.0 equiv) and DMAP (one crystal) were sequentially added to a stirring solution of amine **18** (**V3hh**, 1.0 equiv) in anhydrous dichloromethane (0.04 M) at 0 °C. Acyl chloride (2.0 equiv) was then added dropwise to the mixture, and the reaction mixture was allowed to slowly warm to room temperature and continued to stir overnight (∼19 h). Upon consumption of the starting material (by TLC analysis), the reaction contents were then concentration *in vacuo*, dissolved in a (1:1) 10% w/v aqueous potassium bicarbonate/methanol solution (0.3 M), and allowed to stir at room temperature for 3 to 12 h. After this time, the reaction was quenched with brine and extracted with dichloromethane. The combined organic layers were dried with sodium sulfate, and the crude product was purified by silica gel chromatography.

According to general procedure A, **18** (107 mg, 0.246 mmol) and acetyl chloride (17 μL, 0.246 mmol) were reacted. The crude product was purified by silica gel chromatography using a gradient of 9:1 to 1:3 hexanes/ethyl acetate to yield **20** (**V3ii**), methyl (11*S*,19*S*)-15-acetyl-11-ethyl-19-(4-hydroxyphenyl)-8,15-diazatetracyclo[9.6.2.0^{2,7}.0^{8,18}]nonadeca-1(18),2(7),3,5,9-pentaene-9-carboxylate, as white foam (43.5 mg, 37%). ^{1}H NMR (600 MHz, $C_2Cl_4D_2$ at 100 °C): δ 7.49 (m, 1H), 7.28 (m, 1H), 7.27−7.18 (m, 2H), 7.06 (d, *J* = 8.6 Hz, 2H), 6.76 (d, *J* = 8.6 Hz, 2H), 6.22 (s, 1H), 5.52 (br s, 1H), 4.28 (s, 1H), 4.05 (s, 3H), 3.90 (br m, 2H), 3.13 (br m, 2H), 2.98 (dd, *J* = 13.1, 4.4 Hz, 1H), 2.38 (br m, 1H), 2.19 (s, 3H), 1.84 (ddd, *J* = 15.6, 9.9, 1.8 Hz, 1H), 1.62−1.43 (m, 2H), 1.41 (m, 1H), 1.17 (br m, 1H), 0.94 (br m, 1H), 0.88 (t, *J* = 7.3 Hz, 3H). ^{13}C NMR (151 MHz, $C_2Cl_4D_2$ at 100 °C): δ 172.1, 164.1, 154.7, 137.6, 135.1, 130.4, 129.9, 128.5, 122.3, 120.7, 117.8, 115.3, 112.0, 54.5, 52.9, 52.2, 45.2, 43.2, 33.8, 27.0, 24.2, 21.9, 7.9. Note: four ^{13}C signals were not observed within our spectra (three ^{13}C > 100 ppm and one ^{13}C < 100 ppm). HRMS (ESI): calcd for $C_{29}H_{33}N_2O_4$ $[M + H]^+$, 473.2435; found, 473.2436. $[\alpha]_{20}^{D}$ −32° (*c* 0.40 g/100 mL, CH_2Cl_2).

According to general procedure B, **18** (48.5 mg, 0.113 mmol), dicylcohexyldiimide (23.3 mg, 0.113 mmol), and one crystal of 4-dimethylamiopyridine were reacted. The crude product was purified by silica gel chromatography using a gradient of 9:1 to 1:1 hexanes/ethyl acetate to furnish **21** (**V3jj**), methyl (11*S*,19*S*)-11-ethyl-19-(4-hydroxyphenyl)-15-(6-methoxypyridine-3-carbonyl)-8,15-diazatetracyclo-[9.6.2.0^{2,7}.0^{8,18}]nonadeca-1(18),2(7),3,5,9-pentaene-9-carboxylate (30.5 mg, 48%), as a white solid. ^{1}H NMR (400 MHz, $C_2Cl_4D_2$ at 100 °C): δ 8.13 (s, 1H), 7.41 (d, *J* = 7.7 Hz, 1H), 7.31 (m, 1H), 7.30−7.21 (m, 2H), 7.17 (t, *J* = 7.3 Hz, 1H), 7.11 (d, *J* = 8.2 Hz, 2H), 6.77 (d, *J* = 8.2 Hz, 2H), 6.64 (d, *J* = 8.5 Hz, 1H), 6.25 (s, 1H), 4.80 (br s, 1H), 4.42 (s, 1H), 4.05 (s, 3H), 4.01 (s, 3H), 3.89−3.73 (m, 2H), 3.47 (ddd, *J* = 14.1, 10.6, 3.3 Hz, 1H), 3.17 (ddd, *J* = 14.7, 10.6, 3.7 Hz, 1H), 3.03 (m, 1H), 2.80 (dt, *J* = 14.0, 4.2 Hz, 1H), 1.91−1.41 (m, 4H), 1.24 (sextet, *J* = 7.0 Hz, 1H), 0.90 (t, *J* = 7.3 Hz, 3H), 0.90 (m, 1H; buried under triplet). ^{13}C NMR (101 MHz, $C_2Cl_4D_2$ at 100 °C): δ 171.3, 164.5, 164.0, 154.4, 145.6, 137.3, 137.1, 135.0, 130.3, 130.1, 129.4, 128.6, 126.1, 122.4, 120.8, 118.3, 115.3, 112.0, 111.1, 110.2, 99.5, 53.5, 52.4, 52.2, 50.9, 44.7, 43.7, 32.3, 26.5, 23.6, 21.8, 7.9. HRMS (ESI): calcd for $C_{34}H_{36}N_3O_5$ $[M + H]^+$, 566.2649; found, 566.2650. $[\alpha]_{20}^{D}$ −47° (*c* 0.31 g/100 mL, CH_2Cl_2).

According to general procedure B, **18** (25.9 mg, 0.060 mmol), dicylcohexyldiimide (12.4 mg, 0.060 mmol), and one crystal of 4-dimethylamiopyridine were reacted. The crude product was purified by silica gel chromatography using a gradient of 9:1 hexanes/ethyl acetate to 100% ethyl acetate to 49:1 ethyl acetate/methanol to yield **22** (**V3kk**), methyl (11*S*,19*S*)-11-ethyl-19-(4-hydroxyphenyl)-15-{2-[2-(2-methoxyethoxy)ethoxy]acetyl}-8,15-diazatetracyclo-[9.6.2.0^{2,7}.0^{8,18}]nonadeca-1(18),2(7),3,5,9-pentaene-9-carboxylate (9.9 mg, 28%), as a colorless residue. ^{1}H NMR (400 MHz, $C_2Cl_4D_2$ at 100 °C): δ 7.48 (d, *J* = 7.5 Hz, 1H), 7.27 (d, *J* = 8.1 Hz, 1H), 7.25−7.16 (m, 2H), 7.04 (d, *J* = 8.1 Hz, 2H), 6.74 (d, *J* = 8.2 Hz, 2H), 6.23 (s, 1H), 5.84 (br s, 1H), 4.32−4.13 (m, 2H), 4.26 (s, 1H), 4.05−3.78 (br m, 2H), 4.03 (s, 3H), 3.70−3.56 (m, 6H), 3.55−3.50 (m, 2H), 3.36 (s, 3H), 3.24−3.08 (m, 2H), 3.00 (br m, 1H), 2.44 (br m, 1H), 1.87−1.56 (m, 3H), 1.50 (sextet, *J* = 7.3 Hz, 1H), 1.16 (m, 1H), 0.87 (t, *J* = 7.4 Hz, 3H), 0.84 (m, 1H; partially buried under triplet). ^{13}C NMR (151 MHz, $C_2Cl_4D_2$ at 100 °C): δ 170.9, 164.0, 154.8, 137.5, 135.1, 130.3, 130.1, 130.0, 129.9, 129.4, 128.5, 122.3, 120.7, 117.9, 115.2, 112.0, 71.8, 70.7, 70.3, 70.3, 70.2, 58.5, 53.8, 52.2, 50.9, 44.8, 43.4, 33.4, 26.7, 24.0, 22.0. 7.9. HRMS (ESI): calcd for $C_{34}H_{43}N_2O_7$ $[M + H]^+$, 591.3065; found, 591.3070. $[\alpha]_{20}^{D}$ −34° (*c* 0.53 g/100 mL, CH_2Cl_2).

According to general procedure A, **18** (102 mg, 0.235 mmol) and cylcohexanecarbonyl chloride (31 μL, 0.235 mmol) were reacted. The crude product was purified by silica gel chromatography using a gradient of 99.8:0.2 to 99.5:0.5 chloroform/methanol to yield **23** (**V3ll**), methyl (11*S*,19*S*)-15-cyclohexanecarbonyl-11-ethyl-19-(4-hydroxyphenyl)-8,15-diazatetracyclo[9.6.2.0^{2,7}.0^{8,18}]nonadeca-1(18),2(7),3,5,9-pentaene-9-carboxylate, as white foam (64.4 mg, 51%). ^{1}H NMR (400 MHz, $C_2Cl_4D_2$ at 100 °C): δ 7.50 (d, *J* = 7.3 Hz, 1H), 7.28 (d, *J* = 8.0 Hz, 1H), 7.26−7.18 (m, 2H), 7.05 (d, *J* = 8.1 Hz, 2H), 6.74 (d, *J* = 8.2 Hz, 2H), 6.20 (s, 1H), 4.87 (br s, 1H), 4.27 (s, 1H), 4.04 (s, 3H), 4.00 (br m, 1H), 3.82 (br m, 1H), 3.20 (br m, 1H), 3.14−2.95 (m, 2H), 2.64−2.38 (m, 2H), 1.95−1.08 (m, 15H), 0.89 (t, *J* = 7.4 Hz, 3H), 0.89 (m, 1H; buried under triplet). ^{13}C NMR (151 MHz, $C_2Cl_4D_2$ at 100 °C): δ 177.9, 164.1, 154.5, 137.4, 135.1, 130.5, 130.0, 129.7, 129.4, 128.6, 122.3, 121.0, 120.7, 117.9, 115.2, 112.0,

https://doi.org/10.1021/acsomega.1c02480
ACS Omega 2021, 6, 20455−20470

53.3, 52.2, 51.4, 44.8, 43.4, 41.6, 32.9, 29.9, 28.8, 26.9, 25.7, 25.6, 25.1, 24.6, 22.1, 7.9. HRMS (ESI): calcd for $C_{34}H_{41}N_2O_4$ $[M + H]^+$, 541.3061; found, 541.3064. mp 120−122 °C. $[\alpha]_{20}^{D}$ −69° (*c* 0.14 g/100 mL, CH_2Cl_2).

According to general procedure D, **18** (56.8 mg, 0.132 mmol) and 4-(trifluoromethyl)benzoyl chloride (39.2 μL, 0.264 mmol) were reacted. The crude product was purified by silica gel chromatography using a gradient of 9:1 to 1:1 hexanes/ethyl acetate to yield **24** (**V3mm**), methyl (11*S*,19*S*)-11-ethyl-19-(4-hydroxyphenyl)-15-[4-(trifluoromethyl)-benzoyl]-8,15-diazatetracyclo[9.6.2.$0^{2,7}$.$0^{8,18}$]nonadeca-1-(18),2(7),3,5,9-pentaene-9-carboxylate, as a colorless solid (27.9 mg, 35%). ^{1}H NMR (600 MHz, $C_2Cl_4D_2$ at 100 °C): δ 7.52 (d, *J* = 7.9 Hz, 2H), 7.33 (d, *J* = 8.7 Hz, 2H), 7.27 (dd, *J* = 8.6, 8.0 Hz, 1H), 7.16−7.01 (m, 5H), 6.77 (d, *J* = 8.5 Hz, 2H), 6.25 (s, 1H), 4.73 (s, 1H), 4.39 (s, 1H), 4.06 (s, 3H), 3.75−3.62 (br m, 2H), 3.54 (br dd, *J* = 14.0, 12.0 Hz, 1H), 3.12 (ddd, *J* = 12.5, 10.4, 4.0 Hz, 1H), 3.08−2.80 (br m, 2H), 1.78−1.66 (br m, 2H), 1.59 (br m, 1H), 1.25 (sextet, *J* = 7.3 Hz, 1H), 0.92 (t, *J* = 7.3 Hz, 3H), 0.90 (m, 1H). Note: Due to excessive line broadening in our spectra, we were unable to characterize one proton signal in the upfield aliphatic region (see Supporting Information). ^{13}C NMR (151 MHz, $C_2Cl_4D_2$ at 100 °C): δ 172.1, 164.0, 154.4, 140.6, 137.2, 135.1, 130.9 (d, *J* = 33 Hz), 130.4, 130.2, 130.1, 129.2, 128.7, 126.7, 125.2, 123.6 (q, *J* = 271 Hz), 122.5, 120.9, 118.5, 115.3, 112.0, 110.9, 52.3, 51.0, 50.2, 44.7, 43.6, 31.1, 26.4, 22.9, 21.2, 7.9. ^{19}F NMR (565 MHz, $CDCl_3$): δ −63.36. HRMS (ESI): calcd for $C_{35}H_{34}F_3N_2O_4$ $[M + H]^+$, 603.2465; found, 603.2464. mp 172−174 °C. $[\alpha]_{20}^{D}$ −6° (*c* 0.35 g/100 mL, CH_2Cl_2).

According to general procedure A, **18** (111 mg, 0.257 mmol) and nicotinoyl chloride hydrochloride (46.0 mg, 0.257 mmol) were reacted. The crude product was purified by silica gel chromatography using a gradient of 99:1 to 97.5:2.5 chloroform/methanol to yield **25** (**V3nn**), methyl (11*S*,19*S*)-11-ethyl-19-(4-hydroxyphenyl)-15-(pyridine-3-carbonyl)-8,15-diazatetracyclo[9.6.2.$0^{2,7}$.$0^{8,18}$]nonadeca-1(18),2(7),3,5,9-pentaene-9-carboxylate, as a white solid (52.7 mg, 38%). ^{1}H NMR (600 MHz, $C_2Cl_4D_2$ at 100 °C): δ 8.61 (d, *J* = 3.7 Hz, 1H), 8.47 (br s, 1H), 7.37 (d, *J* = 3.6 Hz, 1H), 7.34−7.29 (m, 2H), 7.25 (dd, *J* = 8.4, 8.0 Hz, 1H), 7.22 (br m, 1H), 7.20−7.13 (m, 2H), 7.10 (d, *J* = 8.2 Hz, 2H), 6.76 (d, *J* = 8.3 Hz, 2H), 6.25 (s, 1H), 4.38 (s, 1H), 4.05 (s, 3H), 3.86−3.67 (br m, 2H), 3.50 (br dd, *J* = 15.2, 12.1 Hz, 1H), 3.13 (m, 1H), 3.04 (br m, 1H), 2.86 (dt, *J* = 14.4, 4.6 Hz, 1H), 1.98−1.63 (br m, 3H), 1.56 (m, 1H), 1.25 (sextet, *J* = 7.4 Hz, 1H), 0.90 (t, *J* = 7.4 Hz, 3H), 0.87 (m, 1H). ^{13}C NMR (151 MHz, $C_2Cl_4D_2$ at 100 °C): δ 170.8, 163.9, 154.5, 149.6, 147.0, 137.3, 135.1, 134.0, 133.2, 130.4, 130.1, 129.9, 129.3, 128.6, 123.2, 122.5, 120.9, 118.4, 115.3, 112.0, 110.9, 52.3, 51.9, 50.1, 44.7, 43.6, 31.8, 26.5, 23.1, 21.5, 7.9. HRMS (ESI): calcd for $C_{33}H_{34}N_3O_4$ $[M + H]^+$, 536.2544; found, 536.2522. $[\alpha]_{20}^{D}$ −43° (*c* 0.18 g/100 mL, CH_2Cl_2).

According to general procedure A, **18** (30.4 mg, 0.071 mmol) and 2-furoyl chloride (7.02 μL, 0.071 mmol) were reacted. The crude product was purified by silica gel chromatography using a gradient of 100% chloroform to 87.5:12.5 chloroform/ethyl acetate to yield **26** (**V3oo**), methyl (11*S*,19*S*)-11-ethyl-15-(furan-2-carbonyl)-19-(4-hydroxyphenyl)-8,15-diazatetracyclo[9.6.2.$0^{2,7}$.$0^{8,18}$]nonadeca-1(18),2-(7),3,5,9-pentaene-9-carboxylate, as white foam (25.7 mg, 69%). ^{1}H NMR (600 MHz, $C_2Cl_4D_2$ at 100 °C): δ 7.54 (s, 1H), 7.49 (d, *J* = 7.6 Hz, 1H), 7.29 (d, *J* = 8.3 Hz, 1H), 7.26−7.18 (m, 2H), 7.10 (d, *J* = 3.4 Hz, 1H), 7.02 (d, *J* = 8.1 Hz, 2H), 6.71 (d, *J* = 8.1 Hz, 2H), 6.56 (dd, *J* = 3.2, 1.5 Hz, 1H), 6.25 (s, 1H), 4.70 (br s, 1H), 4.43 (s, 1H), 4.37 (dt, *J* = 14.2, 3.3 Hz, 1H), 4.25 (dd, *J* = 13.9, 9.0 Hz, 1H), 4.04 (s, 3H), 3.39 (ddd, *J* = 15.5, 11.3, 2.2 Hz, 1H), 3.19 (dd, *J* = 14.6, 13.1 Hz, 1H), 3.00 (m, 1H), 2.44 (d, *J* = 13.5 Hz, 1H), 1.91 (dd, *J* = 15.5, 10.5 Hz, 1H), 1.77−1.57 (m, 2H), 1.44 (sextet, *J* = 7.3 Hz, 1H), 1.14 (sextet, *J* = 7.4 Hz, 1H), 0.94 (m, 1H), 0.85 (t, *J* = 7.4 Hz, 3H). ^{13}C NMR (151 MHz, $C_2Cl_4D_2$ at 100 °C): δ 164.0, 161.7, 154.3, 148.9, 143.6, 137.7, 134.9, 130.8, 130.2, 130.1, 129.5, 128.6, 122.2, 120.6, 117.9, 115.8, 115.1, 112.0, 111.2, 55.4, 53.1, 52.2, 44.9, 43.4, 34.6, 26.7, 24.5, 22.3, 7.9. Note: Despite multiple attempts to characterize all carbon atoms at 100 °C, one ^{13}C signal >100 ppm was not visible. HRMS (ESI): calcd for $C_{32}H_{33}N_2O_5$ $[M + H]^+$, 525.2384; found, 525.2388. mp 141−143 °C. $[\alpha]_{20}^{D}$ −67° (*c* 0.11 g/100 mL, CH_2Cl_2).

According to general procedure A, **18** (101 mg, 0.234 mmol) and 5-pyrimidinecarbonyl chloride (33.5 mg, 0.234 mmol) were reacted. The crude product was purified by silica gel chromatography using a gradient of 99.5:0.5 to 98.2:1.8 chloroform/methanol to yield **27** (**V3pp**), methyl (11*S*,19*S*)-11-ethyl-19-(4-hydroxyphenyl)-15-(pyrimidine-5-carbonyl)-8,15-diazatetracyclo[9.6.2.$0^{2,7}$.$0^{8,18}$]nonadeca-1(18),2(7),3,5,9-pentaene-9-carboxylate, as off-white foam (91.1 mg, 73%). ^{1}H NMR (600 MHz, $C_2Cl_4D_2$ at 100 °C): δ 9.20 (s, 1H), 8.37 (br s, 2H), 7.45−7.30 (m, 2H), 7.26 (dd, *J* = 7.9, 7.4 Hz, 1H), 7.14 (dd, *J* = 7.5, 7.4 Hz, 1H), 7.10 (d, *J* = 8.4 Hz, 2H), 6.77 (d, *J* = 8.5 Hz, 2H), 6.25 (s, 1H), 4.87 (br s, 1H), 4.33 (s, 1H), 4.05 (s, 3H), 3.88−3.49 (br m, 3H), 3.26−2.97 (br m, 2H), 2.90 (dt, *J* = 10.6, 4.8 Hz, 1H), 1.94−1.64 (br m, 3H), 1.56 (m, 1H), 1.27 (sextet, *J* = 7.3 Hz, 1H), 0.91 (t, *J* = 7.4 Hz, 3H), 0.81 (br m, 1H). ^{13}C NMR (151 MHz, $C_2Cl_4D_2$ at 100 °C): δ 168.1, 163.9, 158.5, 154.5, 154.2, 137.1, 135.1, 131.1, 130.4, 130.0, 129.9, 129.2, 128.5, 122.6, 121.0, 118.4, 115.3, 112.0, 110.8, 52.3, 51.9, 49.6, 44.7, 43.6, 31.6, 26.4, 23.0, 21.4, 7.9. HRMS (ESI): calcd for $C_{32}H_{33}N_4O_4$ $[M + H]^+$, 537.2496; found, 537.2505. mp 155−157 °C, decomposed. $[\alpha]_{20}^{D}$ −37° (*c* 0.32 g/100 mL, CH_2Cl_2).

According to general procedure A, **18** (129 mg, 0.299 mmol) and isoxazole-5-carbonyl chloride (29 μL, 0.299 mmol) were reacted. The crude product was purified by silica gel chromatography using a gradient of 100% chloroform to 99:1 chloroform/methanol to yield **28** (**V3qq**), methyl (11*S*,19*S*)-11-ethyl-19-(4-hydroxyphenyl)-15-(1,2-oxazole-5-carbonyl)-8,15-diazatetracyclo[9.6.2.$0^{2,7}$.$0^{8,18}$]nonadeca-1(18),2(7),3,5,9-pentaene-9-carboxylate, as a colorless residue (61.9 mg, 39%). ^{1}H NMR (600 MHz, $C_2Cl_4D_2$ at 100 °C): δ 8.32 (s, 1H), 7.45 (d, *J* = 7.7 Hz, 1H), 7.30 (d, *J* = 8.3 Hz, 1H), 7.25 (dd, *J* = 8.3, 8.0 Hz, 1H), 7.20 (dd, *J* = 8.2, 7.1 Hz, 1H), 7.05 (d, *J* = 8.1 Hz, 2H), 6.73 (d, *J* = 8.2 Hz, 2H), 6.64 (s, 1H), 6.24 (s, 1H), 5.17 (br s, 1H), 4.32 (s, 1H), 4.24 (br m, 1H), 4.12 (m, 1H), 4.05 (s, 3H), 3.34−3.23 (m, 2H), 3.05 (br m, 1H), 2.60 (br m, 1H), 1.86 (br m, 1H), 1.80−1.52 (m, 2H), 1.46 (br m, 1H), 1.19 (sextet, *J* = 7.4 Hz, 1H), 0.94 (br m, 1H), 0.86 (t, *J* = 7.4 Hz, 3H). ^{13}C NMR (151 MHz, $C_2Cl_4D_2$ at 100 °C): δ 164.1, 164.0, 159.9, 154.6, 149.7, 137.5, 135.0, 130.3, 130.2, 129.9, 129.3, 128.4, 122.4, 120.8, 118.0, 115.3, 112.0, 111.4, 106.4, 54.7, 52.5, 52.3, 44.9, 43.3, 33.9, 26.8, 24.1, 21.9, 7.8. HRMS (ESI): calcd for $C_{31}H_{32}N_3O_5$ $[M + H]^+$, 526.2336; found, 526.2332. $[\alpha]_{20}^{D}$ −121° (*c* 0.24 g/100 mL, CH_2Cl_2).

According to general procedure A, **18** (80.5 mg, 0.187 mmol) and pyrrole-2-carbonyl chloride (25.8 mg, 0.187 mmol)

https://doi.org/10.1021/acsomega.1c02480
ACS Omega 2021, 6, 20455−20470

were reacted. The crude product was purified by silica gel chromatography using a gradient of 9:1 to 1:1 hexanes/ethyl acetate to yield **29** (**V3rr**), methyl (11*S*,19*S*)-11-ethyl-19-(4-hydroxyphenyl)-15-(1*H*-pyrrole-2-carbonyl)-8,15-diazatetracyclo[9.6.2.0^{2,7}.0^{8,18}]nonadeca-1(18),2(7),3,5,9-pentaene-9-carboxylate, as a white solid (93 mg, 95%). ^{1}H NMR (600 MHz, $C_2Cl_4D_2$ at 100 °C): δ 9.50 (s, 1H), 7.50 (d, J = 7.5 Hz, 1H), 7.30 (d, J = 7.8 Hz, 1H), 7.25 (dd, J = 8.3, 7.6 Hz, 1H), 7.23 (dd, J = 7.8, 7.3 Hz, 1H), 6.99 (m, 1H, buried), 6.98 (d, J = 8.5 Hz, 2H), 6.69 (m, 1H, buried), 6.68 (d, J = 8.3 Hz, 2H), 6.35 (q, J = 3.2 Hz, 1H), 6.25 (s, 1H), 4.79 (br s, 1H), 4.55 (dq, J = 14.6, 2.0 Hz, 1H), 4.40 (s, 1H), 4.27 (m, 1H), 4.05 (s, 3H), 3.38 (ddd, J = 14.4, 11.4, 2.7 Hz, 1H), 3.24 (dd, J = 14.8, 12.4 Hz, 1H), 3.07 (dd, J = 15.3, 3.7 Hz, 1H), 2.44 (br dd, J = 13.9, 3.2 Hz, 1H), 1.97 (ddd, J = 15.3, 9.8, 2.1 Hz, 1H), 1.82 (m, 1H), 1.67 (m, 1H), 1.44 (sextet, J = 7.4 Hz, 1H), 1.13 (sextet, J = 7.4 Hz, 1H), 0.94 (m, 1H), 0.86 (t, J = 7.4 Hz, 3H). ^{13}C NMR (151 MHz, $C_2Cl_4D_2$ at 100 °C): δ 164.0, 163.7, 154.3, 137.7, 135.0, 130.7, 130.2, 130.0, 129.6, 128.5, 125.5, 122.3, 120.8, 120.7, 117.8, 115.1, 112.0, 112.0, 111.9, 110.2, 55.8, 53.3, 52.2, 44.8, 43.5, 34.7, 26.7, 24.8, 22.6, 7.9. HRMS (ESI): calcd for $C_{32}H_{34}N_3O_4$ [M + H]$^+$, 524.2544; found, 524.2535. mp 160−162 °C. $[\alpha]_{20}^{D}$ −82° (c 0.22 g/100 mL, CH_2Cl_2).

According to general procedure A, **18** (90 mg, 0.21 mmol) and pyridine-2-carbonyl chloride hydrochloride (37 mg, 0.21 mmol) were reacted. The crude product was purified by silica gel chromatography using a gradient of 100% hexanes to 1:4 hexanes/ethyl acetate to yield **30** (**V3ss**), methyl (11*S*,19*S*)-11-ethyl-19-(4-hydroxyphenyl)-15-(pyridine-2-carbonyl)-8,15-diazatetracyclo[9.6.2.0^{2,7}.0^{8,18}]nonadeca-1(18),2(7),3,5,9-pentaene-9-carboxylate, as an off-white solid (48 mg, 43%). ^{1}H NMR (400 MHz, $C_2Cl_4D_2$ at 100 °C): δ 8.62 (dt, J = 4.6, 1.1 Hz, 1H), 7.77 (ddd, J = 8.7, 7.7, 1.7 Hz, 1H), 7.48 (d, J = 7.6 Hz, 1H), 7.40 (m, 1H), 7.35 (ddd, J = 7.6, 4.9, 1.0 Hz, 1H), 7.29 (dt, J = 8.2, 0.7 Hz, 1H), 7.23 (ddd, J = 8.3, 7.0, 1.2 Hz, 1H), 7.20−7.13 (m, 3H), 6.77−6.71 (m, 2H), 6.26 (s, 1H), 5.05 (br s, 1H), 4.61 (s, 1H), 4.17 (ddd, J = 14.0, 9.0, 2.8 Hz, 1H), 4.10 (br m, 1H; buried), 4.05 (s, 3H), 3.51 (m, 1H), 3.20 (ddd, J = 14.8, 11.5, 1.5 Hz, 1H), 2.78 (br m, 1H), 2.51 (br m, 1H), 1.99−1.43 (m, 4H), 1.18 (sextet, J = 7.4 Hz, 1H), 0.97 (m, 1H), 0.86 (t, J = 7.2 Hz, 3H). ^{13}C NMR (126 MHz, $C_2Cl_4D_2$ at 100 °C): δ 170.8, 164.1, 155.2, 154.3, 148.1, 137.9, 136.5, 135.0, 131.1, 130.3, 129.6, 128.7, 124.0, 122.8, 122.1, 120.6, 117.9, 115.1, 111.9, 54.3, 52.8, 52.2, 44.9, 43.4, 34.1, 26.9, 23.9, 22.1, 7.9. Note: Two ^{13}C nuclei are missing within the spectra (>100 ppm) due to significant peak broadening. HRMS (ESI): calcd for $C_{33}H_{34}N_3O_4$ [M + H]$^+$, 536.2544; found, 536.2552. mp 149−151 °C, decomposed. $[\alpha]_{20}^{D}$ −50° (c 0.10 g/100 mL, CH_2Cl_2).

According to general procedure A, **18** (27.7 mg, 0.064 mmol) and isonicotinoyl chloride hydrochloride (8.9 mg, 0.064 mmol) were reacted. The crude product was purified by silica gel chromatography using a gradient of 99.5:0.5 to 9:1 chloroform/methanol to yield **31** (**V3tt**), methyl (11*S*,19*S*)-11-ethyl-19-(4-hydroxyphenyl)-15-(pyridine-4-carbonyl)-8,15-diazatetracyclo[9.6.2.0^{2,7}.0^{8,18}]nonadeca-1(18),2(7),3,5,9-pentaene-9-carboxylate, as a colorless residue (14.4 mg, 42%). ^{1}H NMR (600 MHz, $C_2Cl_4D_2$ at 100 °C): δ 8.52 (d, J = 4.1 Hz, 2H), 7.40−7.30 (m, 2H), 7.27 (dd, J = 9.0, 8.0 Hz, 1H), 7.15 (dd, J = 8.1, 7.4 Hz, 1H), 7.12 (d, J = 8.1 Hz, 2H), 6.87−6.80 (br m, 2H), 6.77 (d, J = 8.1 Hz, 2H), 6.25 (s, 1H), 4.35 (s, 1H), 4.06 (s, 3H), 3.81−3.57 (br m, 2H), 3.51 (m, 1H), 3.24−2.77 (m, 3H), 2.30−1.48 (m, 4H), 1.26 (sextet, J = 7.4 Hz, 1H), 0.92 (t, J = 7.4 Hz, 3H), 0.90 (m, 1H; partially buried). ^{13}C NMR (151 MHz, $C_2Cl_4D_2$ at 100 °C): δ 171.0, 164.0, 154.7, 149.7, 144.5, 137.2, 135.1, 130.4, 130.1, 129.9, 129.2, 128.6, 122.5, 120.9, 120.6, 118.5, 115.3, 112.0, 110.7, 52.3, 50.9, 50.2, 44.7, 43.6, 31.0, 26.4, 22.9, 21.1, 7.9. HRMS (ESI): calcd for $C_{33}H_{34}N_3O_4$ [M + H]$^+$, 536.2544; found, 536.2519. $[\alpha]_{20}^{D}$ −5° (c 0.15 g/100 mL, CH_2Cl_2).

According to general procedure A, **18** (55.6 mg, 0.129 mmol) and 5-chloropyridine-3-carbonyl chloride (22.6 mg, 0.129 mmol) were reacted. The crude product was purified by silica gel chromatography using a gradient of 9:1 to 1:1 hexanes/ethyl acetate to yield **32** (**V3uu**), methyl (11*S*,19*S*)-15-(5-chloropyridine-3-carbonyl)-11-ethyl-19-(4-hydroxyphenyl)-8,15-diazatetracyclo[9.6.2.0^{2,7}.0^{8,18}]nonadeca-1(18),2(7),3,5,9-pentaene-9-carboxylate, as a white solid (35.7 mg, 49%). ^{1}H NMR (600 MHz, $C_2Cl_4D_2$ at 100 °C): δ 8.59 (s, 1H), 8.22 (br s, 1H), 7.40−7.25 (m, 3H), 7.25 (dd, J = 8.8, 7.6 Hz, 1H), 7.15 (dd, J = 8.8, 7.6 Hz, 1H), 7.11 (d, J = 8.5 Hz, 2H), 6.77 (d, J = 8.6 Hz, 2H), 6.25 (s, 1H), 5.29 (br s, 1H), 4.34 (s, 1H), 4.05 (s, 3H), 3.79 (m, 1H), 3.70 (br m, 1H), 3.57 (m, 1H), 3.19−3.01 (m, 2H), 2.86 (dt, J = 14.4, 4.7 Hz, 1H), 1.90−1.61 (br m, 3H), 1.56 (m, 1H), 1.27 (sextet, J = 7.3 Hz, 1H), 0.91 (t, J = 7.4 Hz, 3H), 0.83 (br m, 1H). ^{13}C NMR (151 MHz, $C_2Cl_4D_2$ at 100 °C): δ 169.1, 163.9, 154.6, 148.9, 144.7, 137.1, 135.1, 133.9, 133.7, 131.8, 130.5, 130.1, 129.9, 129.2, 128.4, 122.6, 121.0, 118.3, 115.3, 112.0, 110.7, 52.3, 52.0, 50.2 (br), 44.7, 43.6, 31.9, 26.6, 23.0, 21.5, 7.9. HRMS (ESI): calcd for $C_{33}H_{33}ClN_3O_4$ [M + H]$^+$, 570.2154; found, 570.2156. mp 130−132 °C. $[\alpha]_{20}^{D}$ −7° (c 0.39 g/100 mL, CH_2Cl_2).

According to general procedure A, **18** (48.9 mg, 0.114 mmol) and 5-bromopyridine-3-carbonyl chloride (25.1 mg, 0.114 mmol) were reacted. The crude product was purified by silica gel chromatography using a gradient of 9:1 to 3:1 hexanes/ethyl acetate to yield **33** (**V3vv**), methyl (11*S*,19*S*)-15-(5-bromopyridine-3-carbonyl)-11-ethyl-19-(4-hydroxyphenyl)-8,15-diazatetracyclo[9.6.2.0^{2,7}.0^{8,18}]nonadeca-1(18),2(7),3,5,9-pentaene-9-carboxylate, as a white solid (20.8 mg, 30%). ^{1}H NMR (600 MHz, $C_2Cl_4D_2$ at 100 °C): δ 8.70 (s, 1H), 8.25 (br s, 1H), 7.49 (br m, 1H), 7.37 (br m, 1H), 7.32 (d, J = 7.5 Hz, 1H), 7.26 (dd, J = 8.5, 7.7 Hz, 1H), 7.15 (dd, J = 8.5, 7.4 Hz, 1H), 7.11 (d, J = 8.2 Hz, 2H), 6.77 (d, J = 8.2 Hz, 2H), 6.25 (s, 1H), 4.88 (br s, 1H), 4.35 (s, 1H), 4.05 (s, 3H), 3.80 (m, 1H), 3.70 (m, 1H), 3.56 (m, 1H), 3.23−2.99 (br m, 2H), 2.83 (m, 1H), 1.89−1.62 (br m, 3H), 1.56 (m, 1H), 1.27 (sextet, J = 7.3 Hz, 1H), 0.92 (t, J = 7.4 Hz, 3H), 0.84 (m, 1H). ^{13}C NMR (151 MHz, $C_2Cl_4D_2$ at 100 °C): δ 169.0, 163.9, 154.5, 151.1, 145.0, 137.1, 136.5, 135.1, 134.3, 133.7, 130.5, 130.1, 129.2, 128.5, 122.6, 121.0, 120.4, 118.3, 115.3, 112.0, 110.8, 52.3, 52.2, 50.1 (br), 44.7, 43.6, 31.9, 26.6, 23.0, 21.6, 7.9. HRMS (ESI): calcd for $C_{33}H_{33}BrN_3O_4$ [M + H]$^+$, 614.1649; found, 614.1670. mp 123−125 °C. $[\alpha]_{20}^{D}$ −13° (c 0.12 g/100 mL, CH_2Cl_2).

According to general procedure A, **18** (21.7 mg, 0.050 mmol) and benzoyl chloride (5.80 μL, 0.050 mmol) were reacted. The crude product was purified by silica gel chromatography using a gradient of 99.5:0.5 to 99:1 chloroform/methanol to yield **34** (**V3ww**), methyl (11*S*,19*S*)-15-benzoyl-11-ethyl-19-(4-hydroxyphenyl)-8,15-diazatetracyclo[9.6.2.0^{2,7}.0^{8,18}]nonadeca-1(18),2(7),3,5,9-pentaene-9-carboxylate, as a colorless residue (17.2 mg, 64%). ^{1}H NMR (600 MHz, $C_2Cl_4D_2$ at 100 °C): δ 7.43−7.36 (m, 2H), 7.36−7.29 (m, 3H), 7.25 (dd, J = 8.3, 7.9 Hz, 1H), 7.20−7.15

https://doi.org/10.1021/acsomega.1c02480
ACS Omega 2021, 6, 20455−20470

(m, 3H), 7.13 (d, J = 8.6 Hz, 2H), 6.77 (d, J = 8.6 Hz, 2H), 6.25 (s, 1H), 4.80 (br s, 1H), 4.46 (s, 1H), 4.05 (s, 3H), 3.91−3.74 (br m, 2H), 3.40 (ddd, J = 14.8, 9.5, 2.2 Hz, 1H), 3.15 (ddd, J = 15.8, 10.7, 3.2 Hz, 1H), 2.95 (br m, 1H), 2.76 (m, 1H), 1.86−1.63 (m, 3H), 1.56 (m, 1H), 1.23 (sextet, J = 7.4 Hz, 1H), 0.94 (m, 1H), 0.91 (t, J = 7.4 Hz, 3H). ^{13}C NMR (151 MHz, $C_2Cl_4D_2$ at 100 °C): δ 173.5, 164.0, 154.4, 137.3, 137.3, 135.1, 130.4, 130.3, 130.1, 129.4, 129.0, 128.7, 128.2, 126.4, 122.3, 120.8, 118.4, 115.2, 111.9, 111.3, 52.5, 52.2, 51.1, 44.8, 43.7, 32.4, 26.5, 23.6, 21.8, 7.9. HRMS (ESI): calcd for $C_{34}H_{35}N_2O_4$ $[M + H]^+$, 535.2591; found, 535.2614. $[\alpha]_{20}^{D}$ −26° (c 0.10 g/100 mL, CH_2Cl_2).

Synthesis of ***35*** *(**V4h**).* Vincamine (802.1 mg, 2.26 mmol) was added to a flame-dried microwave flask and dissolved in DMF (17.5 mL). A 3.0 M solution of cyanogen bromide in dichloromethane (2.30 mL, 6.79 mmol) was added dropwise to the resulting solution. The reaction was subjected to microwave irradiation at 100 °C for 3 min. The mixture was then cooled to room temperature, diluted with ethyl acetate, and quenched with brine (3 × 100 mL) and transferred to a separatory funnel for extraction. The organic layer was then collected, dried with sodium sulfate, filtered, and concentrated *in vacuo*. The crude material was then purified *via* column chromatography using a gradient of 100% chloroform to 24:1 chloroform/acetone to yield **35** (**V4h**) as a white solid (520 mg, 50%). ^{1}H NMR (600 MHz, $CDCl_3$): δ 7.58 (dd, J = 7.0, 1.0 Hz, 1H), 7.22 (dd, J = 7.6, 0.9 Hz, 1H), 7.21−7.14 (m, 2H), 4.52 (s, 1H), 4.36 (s, 1H), 3.71 (s, 3H), 3.70−3.61 (m, 2H), 3.49−3.38 (m, 2H), 3.31−3.21 (m, 2H), 2.45 (d, J = 14.8 Hz, 1H), 2.29 (d, J = 14.8 Hz, 1H), 2.00 (m, 1H), 1.78 (m, 1H), 1.71−1.63 (m, 2H), 1.59 (pentet, J = 7.5 Hz, 1H), 1.54 (m, 1H), 0.85 (t, J = 7.5 Hz, 3H). ^{13}C NMR (151 MHz, $CDCl_3$): δ 172.9, 135.4, 128.5, 128.2, 123.5, 121.0, 119.0, 118.2, 114.2, 111.8, 82.4, 59.8, 54.2, 48.0, 40.9, 36.3, 32.3, 29.4, 29.1, 28.5, 19.8, 7.3. HRMS (ESI): calcd for $C_{22}H_{26}BrN_3O_3Na$ $[M + Na]^+$, 482.1050; found, 482.1071. mp 155−157 °C. $[\alpha]_{20}^{D}$ +4° (c 0.40 g/100 mL, CH_2Cl_2). Extensive 2D NMR (COSY, HSQC, and HMBC) and NOE experiments were performed on this compound and can be viewed in the Supporting Information. Note: We found this reaction to be sensitive to water and the addition of 4 Å of molecular sieves increased the yield of **35** (**V4h**). In addition, **35** can be purified *via* column chromatography using hexanes/ethyl acetate solvent systems to elute.

Synthesis of ***36*** *(**V4i**).* Compound **35** (**V4h**) (203 mg, 0.441 mmol) was added to a flame-dried microwave flask and dissolved in DMF (4.41 mL). Sodium azide (230 mg, 3.53 mmol) was then added to the resulting solution, which was subjected to microwave irradiation at 100 °C for 4 min. The resulting mixture was allowed to cool to room temperature before being diluted with ethyl acetate and quenched with brine (3 × 50 mL). The contents were then transferred to a separatory funnel, and the organic layer was collected, dried with sodium sulfate, filtered, and concentrated *in vacuo*. The crude material was then purified *via* column chromatography using a gradient of 100% chloroform to 49:1 chloroform/acetone to yield **36** (**V4i**) as a white solid (111.4 mg, 60%). ^{1}H NMR (400 MHz, $CDCl_3$): δ 7.58 (m, 1H), 7.23−7.12 (m, 3H), 4.73 (s, 1H), 4.19 (d, J = 1.4 Hz, 1H), 3.82 (s, 3H), 3.72 (ddd, J = 12.2, 7.0, 5.8 Hz, 1H), 3.64−3.53 (m, 2H), 3.25 (td, J = 12.6, 3.0 Hz, 1H), 3.14−3.06 (m, 2H), 2.98 (d, J = 14.2 Hz, 1H), 1.97−1.82 (m, 3H), 1.75−1.63 (m, 2H), 1.43 (td, J = 14.2, 6.5 Hz, 1H), 1.18 (sextet, J = 7.4 Hz, 1H), 0.91 (t, J = 7.4 Hz, 3H). ^{13}C NMR (101 MHz, $CDCl_3$): δ 174.6, 135.0, 128.4, 128.0, 123.8, 120.9, 119.6, 116.5, 114.3, 111.4, 82.2, 57.8, 54.8, 51.6, 51.0, 35.4, 35.1, 32.9, 30.1, 24.5, 20.4, 7.3. HRMS (ESI): calcd for $C_{22}H_{26}N_6O_3Na$ $[M + Na]^+$, 445.1959; found, 445.1979. mp 127−129 °C. $[\alpha]_{20}^{D}$ −8° (c 0.91 g/100 mL, CH_2Cl_2).

Determination of Solubility and Chemical Stability for Analogue 30 (V3ss). *Solubility.* Compound **30** (**3Vss**) was determined to have 100 mM (highest concentration tested) solubility in biological grade DMSO. The 100 mM solution of **30** in DMSO was then diluted to a 10 mM solution for additional solubility and chemical stability studies. To determine the water solubility of compound **30**, 5 μL of the 10 mM DMSO solution was added to an Eppendorf tube before PBS buffer (495 μL) was slowly titrated in to give a 100 μM solution (highest concentration tested). The resulting aqueous solution of **30** remained completely transparent over 24 h and was compared to a PBS standard.

Chemical Stability. Two separate aqueous solutions of **30** were prepared at 100 μM (15 mL). In the first solution, 14.85 mL of acidified (pH = 1.95) PBS buffer was added to 150 μL of a 10 mM stock solution of **30** in DMSO. In the second solution, 14.85 mL of PBS buffer (pH = 7.4) was added to 150 μL of the 10 mM stock solution of **30** in DMSO. Each 100 μM solution was allowed to stir at room temperature overnight. In both the acidified and neutral solutions, a small amount of precipitate was formed overnight. After 24 h, the solutions were placed inside a 37 °C chamber for an additional 24 h. At the 48 h time point, the appearance of both solutions looked similar to the 24 h time point and both were extracted using ethyl acetate. TLC at the 24 and 48 h time point revealed no degradation of **30**. ^{1}H NMR of the recovered solids from both solutions confirmed that **30** remained intact and was stable in the neutral and acidic solutions for up to 48 h.

■ ASSOCIATED CONTENT

Supporting Information

The Supporting Information is available free of charge at https://pubs.acs.org/doi/10.1021/acsomega.1c02480.

Dose−response curves for vincamine-derived antiplasmodial agents against chloroquine-resistant (Dd2) and chloroquine-sensitive (3D7) cells, kill kinetics, stage-specific activity for positive controls, NMR spectra (^{1}H and ^{13}C NMR spectra, select 2-D NMR) for new compounds, and purity analysis (LC traces) for compounds evaluated in biological assays (PDF)

■ AUTHOR INFORMATION

Corresponding Authors

Debopam Chakrabarti − *Division of Molecular Microbiology, Burnett School of Biomedical Sciences, University of Central Florida, Orlando, Florida 32826, United States;* orcid.org/0000-0002-4554-3119; Phone: (407) 882-2256; Email: dchak@ucf.edu

Robert William Huigens III − *Department of Medicinal Chemistry, Center for Natural Products, Drug Discovery and Development (CNPD3), University of Florida, Gainesville, Florida 32610, United States;* orcid.org/0000-0003-3811-2721; Phone: (352) 273-7718; Email: rhuigens@cop.ufl.edu

Authors

Verrill M. Norwood IV − *Department of Medicinal Chemistry, Center for Natural Products, Drug Discovery and Development (CNPD3), University of Florida, Gainesville, Florida 32610, United States*

Claribel Murillo-Solano − *Division of Molecular Microbiology, Burnett School of Biomedical Sciences, University of Central Florida, Orlando, Florida 32826, United States*

Michael G. Goertzen II − *Department of Medicinal Chemistry, Center for Natural Products, Drug Discovery and Development (CNPD3), University of Florida, Gainesville, Florida 32610, United States;* orcid.org/0000-0003-4005-6685

Beau R. Brummel − *Department of Medicinal Chemistry, Center for Natural Products, Drug Discovery and Development (CNPD3), University of Florida, Gainesville, Florida 32610, United States;* orcid.org/0000-0002-5247-9418

David L. Perry − *Division of Molecular Microbiology, Burnett School of Biomedical Sciences, University of Central Florida, Orlando, Florida 32826, United States*

James R. Rocca − *Department of Medicinal Chemistry, Center for Natural Products, Drug Discovery and Development (CNPD3), University of Florida, Gainesville, Florida 32610, United States; McKnight Brain Institute, J H Miller Health Center, University of Florida, Gainesville, Florida 32610, United States*

Complete contact information is available at: https://pubs.acs.org/10.1021/acsomega.1c02480

Notes

The authors declare no competing financial interest.

■ ACKNOWLEDGMENTS

We acknowledge the University of Florida and the National Institute for General Medical Sciences of the National Institutes of Health for providing support for this work (R35GM128621 to R.W.H.). M.G.G. II was supported by the NIH/NIGMS T32GM136583 "Chemistry-Biology Interface Training Program at the University of Florida". The National High Magnetic Field Laboratory supported a portion of these NMR studies at the Advanced Magnetic Resonance Imaging and Spectroscopy (AMRIS) Facility (McKnight Brain Institute at the University of Florida; supported by National Science Foundation Cooperative Agreement No. DMR-1157490 and the State of Florida). All high resolution mass spectra were obtained for new compounds from the University of Florida's Mass Spectrometry Research and Education Center and supported by NIH S10 OD021758-01A1.

■ ABBREVIATIONS

3D7, chloroquine-sensitive *P. falciparum* strain; ACTs, artemisinin-based combination therapies; Ac_2O, acetic anhydride; °C, degrees Celsius; $CHCl_3$, chloroform; CH_2Cl_2, dichloromethane; Dd2, chloroquine-resistant *P. falciparum* strain; DHA, dihyroartemisinin; DCC, dicyclohexylcarbodiimide; DMAP, 4-dimethylaminopyridine; DMF, *N*,*N*′-dimethylformamide; DMSO, dimethylsulfoxide; EC_{50}, concentration of a drug that gives half-maximal response; h, hour; HCl, hydrochloric acid; HepG2, a human liver cancer cell line; HPI, hours postinvasion; K_2CO_3, potassium carbonate; MeOH, methanol; NMR, nuclear magnetic resonance; PBS, phosphate-buffered saline; PhMe, toluene; PhOH, phenol; *p*-TSA, *para*-toluenesulfonic acid; RCO_2H, carboxylic acid; RCOCl, acyl chloride; SAR, structure−activity relationship; SI, selectivity index; TLC, thin-layer chromatography; μM, micromolar; V, vincamine; V3, V3 scaffold series of ring-distortion analogues; WHO, World Health Organization

■ REFERENCES

(1) Blasco, B.; Leroy, D.; Fidock, D. A. Antimalarial drug resistance: linking *Plasmodium falciparum* parasite biology to the clinic. *Nat. Med.* **2017**, *23*, 917−928.

(2) Cowman, A. F.; Healer, J.; Marapana, D.; Marsh, K. Malaria: biology and disease. *Cell* **2016**, *167*, 610−624.

(3) Shibeshi, M. A.; Kifle, Z. D.; Atnafie, S. A. Antimalarial drug resistance and novel targets for antimalarial drug discovery. *Infect. Drug Resist.* **2020**, *13*, 4047−4060.

(4) WHO *World Malaria Report*, 2020.

(5) Grimberg, B. T.; Mehlotra, R. K. Expanding the antimalarial drug arsenal − now, but how? *Pharmaceuticals* **2011**, *4*, 681−712.

(6) Escalante, A. A.; Smith, D. L.; Kim, Y. The dynamics of mutations associated with anti-malarial drug resistance in *Plasmodium falciparum*. *Trends Parasitol.* **2009**, *25*, 557−563.

(7) Cui, W. WHO urges the phasing out of artemisinin based monotherapy for malaria to reduce resistance. *Br. Med. J.* **2011**, *342*, d2793.

(8) Ashley, E. A.; Dhorda, M.; Fairhurst, R. M.; Amaratunga, C.; Lim, P.; Suon, S.; Sreng, S.; Anderson, J. M.; Mao, S.; Sam, B.; Sopha, C.; Chuor, C. M.; Nguon, C.; Sovannaroth, S.; Pukrittayakamee, S.; Jittamala, P.; Chotivanich, K.; Chutasmit, K.; Suchatsoonthorn, C.; Runcharoen, R.; Hien, T. T.; Thuy-Nhien, N. T.; Thanh, N. V.; Phu, N. H.; Htut, Y.; Han, K.-T.; Aye, K. H.; Mokuolu, O. A.; Olaosebikan, R. R.; Folaranmi, O. O.; Mayxay, M.; Khanthavong, M.; Hongvanthong, B.; Newton, P. N.; Onyamboko, M. A.; Fanello, C. I.; Tshefu, A. K.; Mishra, N.; Valecha, N.; Phyo, A. P.; Nosten, F.; Yi, P.; Tripura, R.; Borrmann, S.; Bashraheil, M.; Peshu, J.; Faiz, M. A.; Ghose, A.; Hossain, M. A.; Samad, R.; Rahman, M. R.; Hasan, M. M.; Islam, A.; Miotto, O.; Amato, R.; MacInnis, B.; Stalker, J.; Kwiatkowski, D. P.; Bozdech, Z.; Jeeyapant, A.; Cheah, P. Y.; Sakulthaew, T.; Chalk, J.; Intharabut, B.; Silamut, K.; Lee, S. J.; Vihokhern, B.; Kunasol, C.; Imwong, M.; Tarning, J.; Taylor, W. J.; Yeung, S.; Woodrow, C. J.; Flegg, J. A.; Das, D.; Smith, J.; Venkatesan, M.; Plowe, C. V.; Stepniewska, K.; Guerin, P. J.; Dondorp, A. M.; Day, N. P.; White, N. J. Tracking resistance to artemisinin collaboration (TRAC). Spread of artemisinin resistance in *Plasmodium falciparum* malaria. *N. Engl. J. Med.* **2014**, *371*, 411−423.

(9) Flannery, E. L.; Chatterjee, A. K.; Winzeler, E. A. Antimalarial drug discovery − approaches and progress towards new medicines. *Nat. Rev. Microbiol.* **2013**, *11*, 849−862.

(10) Burrows, J. N.; Duparc, S.; Gutteridge, W. E.; Hooft van Huijsduijnen, R.; Kaszubska, W.; Macintyre, F.; Mazzuri, S.; Möhrle, J. J.; Wells, T. N. C. New developments in anti-malarial target candidate and product profiles. *Malar. J.* **2017**, *16*, 26.

(11) Paciaroni, N. G.; Perry, D. L.; Norwood, V. M.; Murillo-Solano, C.; Collins, J.; Tenneti, S.; Chakrabarti, D.; Huigens III, R. W. Re-engineering of yohimbine's biological activity through ring distortion: identification and structure−activity relationships of a new class of antiplasmodial agents. *ACS Infect. Dis.* **2020**, *6*, 159−167.

(12) Newman, D. J.; Cragg, G. M. Natural products as sources of new drugs over the nearly four decades from 01/1981 to 09/2019. *J. Nat. Prod.* **2020**, *83*, 770−803.

(13) Carlson, E. E. Natural products as chemical probes. *ACS Chem. Biol.* **2010**, *5*, 639−653.

(14) Böttcher, T.; Pitscheider, M.; Sieber, S. A. Natural products and their biological targets: proteomic and metabolomics labelling strategies. *Angew. Chem., Int. Ed.* **2010**, *49*, 2680−2698.

(15) Chen, X.; Wang, Y.; Ma, N.; Tian, J.; Shao, Y.; Zhu, B.; Wong, Y. K.; Liang, Z.; Zou, C.; Wang, J. Target identification of natural

medicine with chemical proteomics approach: probe synthesis, target fishing and protein identification. *Signal Transduction Targeted Ther.* **2020**, *5*, 72.
(16) Kaserer, T.; Lantero, A.; Schmidhammer, H.; Spetea, M.; Schuster, D. μ Opioid receptor: novel antagonists and structural modeling. *Sci. Rep.* **2016**, *6*, 21548.
(17) Knox, J. R.; Pratt, R. F. Different modes of vancomycin and D-alanyl-D-alanine peptidase binding to cell wall peptide and a posible role for the vancomycin resistance protein. *Antimicrob. Agents Chemother.* **1990**, *34*, 1342−1347.
(18) Zewail-Foote, M.; Hurley, L. H. Differential rates of reversibility of ecteinascidin 743-DNA covalent adducts from different sequences lead to migration to favored bonding sites. *J. Am. Chem. Soc.* **2001**, *123*, 6485−6495.
(19) Brodersen, D. E.; Clemons, W. M.; Carter, A. P.; Morgan-Warren, R. J.; Wimberly, B. T.; Ramakrishnan, V. The structural basis for the action of the antibiotics tetracycline, pactamycin, and hygromycin B on the 30S ribosomal subunit. *Cell* **2000**, *103*, 1143−1154.
(20) Paciaroni, N. G.; Ratnayake, R.; Matthews, J. H.; Norwood, V. M.; Arnold, A. C.; Dang, L. H.; Luesch, H.; Huigens III, R. W. A tryptoline ring-distortion strategy leads to complex and diverse biologically active molecules from the indole alkaloid yohimbine. *Chem.—Eur. J.* **2017**, *23*, 4327.
(21) Norwood, V. M.; Huigens III, R. W. Harnessing the chemistry of the indole heterocycle to drive discoveries in biology and medicine. *ChemBioChem* **2019**, *20*, 2273−2297.
(22) Paciaroni, N. G.; Norwood, V. M.; Garcia, D. E.; Huigens III, R. W. Microwave-enhanced, stereospecific ring-closure of medium-ring cyanamide ethers to yohimbine. *Tetrahedron Lett.* **2019**, *60*, 1182−1185.
(23) Norwood, V. M.; Brice-Tutt, A. C.; Eans, S. O.; Stacy, H. M.; Shi, G.; Ratnayake, R.; Rocca, J. R.; Abboud, K. A.; Li, C.; Luesch, H.; McLaughlin, J. P.; Huigens III, R. W. Preventing morphine-seeking behavior through the re-engineering of vincamine's biological activity. *J. Med. Chem.* **2020**, *63*, 5119−5138.
(24) Paciaroni, N. G.; Norwood, V. M.; Ratnayake, R.; Luesch, H.; Huigens III, R. W. Yohimbine as a starting point to access diverse natural product-like agents with re-programmed activities against cancer-relevant GPCR targets. *Bioorg. Med. Chem.* **2020**, *28*, 115546.
(25) Schreiber, S. L. Organic Chemistry: Molecular Diversity by Design. *Nature* **2009**, *457*, 153−154.
(26) Galloway, W. R. J. D.; Isidro-Llobet, A.; Spring, D. R. Diversity-oriented synthesis as a tool for the discovery of novel biologically active small molecules. *Nat. Commun.* **2010**, *1*, 80.
(27) Shang, S.; Tan, D. S. Advancing chemistry and biology through diversity-oriented synthesis of natural product-like libraries. *Curr. Opin. Chem. Biol.* **2005**, *9*, 248−258.
(28) Wetzel, S.; Bon, R. S.; Kumar, K.; Waldmann, H. Biology-Oriented Synthesis. *Angew. Chem., Int. Ed.* **2011**, *50*, 10800−10826.
(29) van Hattum, H.; Waldmann, H. Biology-oriented synthesis: harnessing the power of evolution. *J. Am. Chem. Soc.* **2014**, *136*, 11853−11859.
(30) Swinney, D. C.; Anthony, J. How were new medicines discovered? *Nat. Rev. Drug Discovery* **2011**, *10*, 507−519.
(31) Macarron, R.; Banks, M. N.; Bojanic, D.; Burns, D. J.; Cirovic, D. A.; Garyantes, T.; Green, D. V. S.; Hertzberg, R. P.; Janzen, W. P.; Paslay, J. W.; Schopfer, U.; Sittampalam, G. S. Impact of high-throughput screening on biomedical research. *Nat. Rev. Drug Discovery* **2011**, *10*, 188−195.
(32) Hughes, J.; Rees, S.; Kalindjian, S.; Philpott, K. Principles of early drug discovery. *Br. J. Pharmacol.* **2011**, *162*, 1239−1249.
(33) Heidebrecht, R. W.; Mulrooney, C.; Austin, C. P.; Barker, R. H.; Beaudoin, J. A.; Cheng, K. C.-C.; Comer, E.; Dandapani, S.; Dick, J.; Duvall, J. R.; Ekland, E. H.; Fidock, D. A.; Fitzgerald, M. E.; Foley, M.; Guha, R.; Hinkson, P.; Kramer, M.; Lukens, A. K.; Masi, D.; Marcaurelle, L. A.; Su, X.-Z.; Thomas, C. J.; Weïwer, M.; Wiegand, R. C.; Wirth, D.; Xia, M.; Yuan, J.; Zhao, J.; Palmer, M.; Munoz, B.; Schreiber, S. Diversity-oriented synthesis yields a novel lead for the treatment of malaria. *ACS Med. Chem. Lett.* **2012**, *3*, 112−117.
(34) Comer, E.; Beaudoin, J. A.; Kato, N.; Fitzgerald, M. E.; Heidebrecht, R. W.; Lee, M. d.; Masi, D.; Mercier, M.; Mulrooney, C.; Muncipinto, G.; Rowley, A.; Crespo-Llado, K.; Serrano, A. E.; Lukens, A. K.; Wiegand, R. C.; Wirth, D. F.; Palmer, M. A.; Foley, M. A.; Munoz, B.; Scherer, C. A.; Duvall, J. R.; Schreiber, S. L. Diversity-oriented synthesis-facilitated medicinal chemistry: toward the development of novel antimalarial agents. *J. Med. Chem.* **2014**, *57*, 8496−8502.
(35) Kato, N.; Comer, E.; Sakata-Kato, T.; Sharma, A.; Sharma, M.; Maetani, M.; Bastien, J.; Brancucci, N. M.; Bittker, J. A.; Corey, V.; Clarke, D.; Derbyshire, E. R.; Dornan, G. L.; Duffy, S.; Eckley, S.; Itoe, M. A.; Koolen, K. M. J.; Lewis, T. A.; Lui, P. S.; Lukens, A. K.; Lund, E.; March, S.; Meibalan, E.; Meier, B. C.; McPhail, J. A.; Mitasev, B.; Moss, E. L.; Sayes, M.; Van Gessel, Y.; Wawer, M. J.; Yoshinaga, T.; Zeeman, A.-M.; Avery, V. M.; Bhatia, S. N.; Burke, J. E.; Catteruccia, F.; Clardy, J. C.; Clemons, P. A.; Dechering, K. J.; Duvall, J. R.; Foley, M. A.; Gusovsky, F.; Kocken, C. H. M.; Marti, M.; Morningstar, M. L.; Munoz, B.; Neafsey, D. E.; Sharma, A.; Winzeler, E. A.; Wirth, D. F.; Scherer, C. A.; Schreiber, S. L. Diversity-oriented synthesis yields novel multistage antimalarial inhibitors. *Nature* **2016**, *538*, 344−349.
(36) Huigens III, R. W.; Morrison, K. C.; Hicklin, R. W.; Flood Jr, T. A.; Richter, M. F.; Hergenrother, P. J. A ring-distortion strategy to construct stereochemically complex and structurally diverse compounds from natural products. *Nat. Chem.* **2013**, *5*, 195−202.
(37) Ross, S. P.; Hoye, T. R. Reactions of hexadehydro-Diels-Alder benzynes with structurally complex multifunctional natural products. *Nat. Chem.* **2017**, *9*, 523−530.
(38) Charaschanya, M.; Aubé, J. Reagent-controlled regiodivergent ring expansions of steroids. *Nat. Commun.* **2018**, *9*, 934.
(39) Llabani, E.; Hicklin, R. W.; Lee, H. Y.; Motika, S. E.; Crawford, L. A.; Weerapana, E.; Hergenrother, P. J. Diverse compounds from pleuromutilin lead to a thioredoxin inhibitor and inducer of ferroptosis. *Nat. Chem.* **2019**, *11*, 521−532.
(40) Rafferty, R. J.; Hicklin, R. W.; Maloof, K. A.; Hergenrother, P. J. Synthesis of complex and diverse compounds through ring distortion of abietic acid. *Angew. Chem., Int. Ed.* **2014**, *53*, 220−224.
(41) Tasker, S. Z.; Cowfer, A. E.; Hergenrother, P. J. Preparation of structurally diverse compounds from the natural product lycorine. *Org. Lett.* **2018**, *20*, 5894−5898.
(42) Hicklin, R. W.; López Silva, T. L.; Hergenrother, P. J. Synthesis of bridged oxafenestranes from pleuromutilin. *Angew. Chem., Int. Ed.* **2014**, *53*, 9880−9883.
(43) Garcia, A.; Drown, B. S.; Hergenrother, P. J. Access to a structurally complex compound collection via ring distortion of the alkaloid sinomenine. *Org. Lett.* **2016**, *18*, 4852−4855.
(44) Smilkstein, M.; Sriwilaijaroen, N.; Kelly, J. X.; Wilairat, P.; Riscoe, M. Simple and inexpensive fluorescence-based technique for high-throughput antimalarial drug screening. *Antimicrob. Agents Chemother.* **2004**, *48*, 1803−1806.
(45) Bennett, T. N.; Paguio, M.; Gligorijevic, B.; Seudieu, C.; Kosar, A. D.; Davidson, E.; Roepe, P. D. Novel, rapid, and inexpensive cell-based quantification of antimalarial drug efficacy. *Antimicrob. Agents Chemother.* **2004**, *48*, 1807−1810.
(46) Johnson, J. D.; Dennull, R. A.; Gerena, L.; Lopez-Sanchez, M.; Roncal, N. E.; Waters, N. C. Assessment and continued validation of the malaria SYBR green I-based fluorescence assay for use in malaria drug screening. *Antimicrob. Agents Chemother.* **2007**, *51*, 1926−1933.
(47) Roberts, B. F.; Iyamu, I. D.; Lee, S.; Lee, E.; Ayong, L.; Kyle, D. E.; Yuan, Y.; Manetsch, R.; Chakrabarti, D. Spirocyclic chromanes exhibit antiplasmodial activities and inhibit all intraerythrocytic life cycle stages. *Int. J. Parasitol.* **2016**, *6*, 85−92.
(48) Roberts, B. F.; Zheng, Y.; Cleaveland, J.; Lee, S.; Lee, E.; Ayong, L.; Yuan, Y.; Chakrabarti, D. 4-Nitro styrylquinoline is an antimalarial inhibiting multiple stages of *Plasmodium falciparum* asexual life cycle. *Int. J. Parasitol.* **2017**, *7*, 120−129.

https://doi.org/10.1021/acsomega.1c02480
ACS Omega 2021, 6, 20455−20470

(49) Bozdech, Z.; Zhu, J.; Joachimiak, M. P.; Cohen, F. E.; Pulliam, B.; DeRisi, J. L. Expression profiling of the schizont and trophozoite stages of *Plasmodium falciparum* with a long-oligonucleotide microarray. *Genome Biol.* **2003**, *4*, R9.
(50) Lebl, T.; Lorion, M. M.; Jones, A. M.; Philp, D.; Westwood, N. J. Synthesis and characterisaton of medium-sized ring systems by oxidative cleavage. Part 2: Insights from the study of ring expanded analogues. *Tetrahedron* **2010**, *66*, 9694−9702.
(51) Guerriero, A.; D'Ambrosio, M.; Pietra, F. Slowly interconverting conformers of the briarane diterpenoids verecynarmin B, C, and D, isolated from the nudibranch mollusc *Armina maculata* and the pennatulacean octocoral *Veretillum cynomorium* of East Pyrenean waters. *Helv. Chim. Acta* **1988**, *71*, 472−485.
(52) Bain, A. D.; Bell, R. A.; Fletcher, D. A.; Hazendonk, P.; Maharajh, R. A.; Rigby, S.; Valliant, J. F. NMR studies of chemical exchange amongst five conformers of a ten-membered ring compound containing two amide bonds and a disulfide. *J. Chem. Soc., Perkin Trans. 2* **1999**, 1447−1454.

https://doi.org/10.1021/acsomega.1c02480
ACS Omega 2021, 6, 20455−20470